REPORT DOCUMENTATION PAGE

The public reporting burden for this collection of information is estimated to average 1 hour per response, including the time for reviewing instructions, searching existing data sources, gathering and maintaining the data needed, and completing and reviewing the collection of information. Send comments regarding this burden estimate or any other aspect of this collection of information, including suggestions for reducing the burden, to Department of Defense, Washington Headquarters Services, Directorate for Information Operations and Reports (0704-0188), 1215 Jefferson Davis Highway, Suite 1204, Arlington, VA 22202-4302. Respondents should be aware that notwithstanding any other provision of law, no person shall be subject to any penalty for failing to comply with a collection of information if it does not display a currently valid OMB control number.
PLEASE DO NOT RETURN YOUR FORM TO THE ABOVE ADDRESS.

1. REPORT DATE (DD-MM-YYYY)	2. REPORT TYPE	3. DATES COVERED (From - To)
07/17/2014	Final Technical Report	03/01/2012 - 03/31/2014

4. TITLE AND SUBTITLE

NGIPS Early Design Space Assessment

5a. CONTRACT NUMBER

5b. GRANT NUMBER

N00014-12-1-0426

5c. PROGRAM ELEMENT NUMBER

6. AUTHOR(S)

Cramer, Aaron, M.

5d. PROJECT NUMBER

5e. TASK NUMBER

5f. WORK UNIT NUMBER

7. PERFORMING ORGANIZATION NAME(S) AND ADDRESS(ES)

University of Kentucky Research Foundation
201 Kinkead Hall
Lexington, KY 40506-0057

8. PERFORMING ORGANIZATION REPORT NUMBER

9. SPONSORING/MONITORING AGENCY NAME(S) AND ADDRESS(ES)

Office of Naval Research
875 North Randolph Street
Arlington, VA 22203-1995

10. SPONSOR/MONITOR'S ACRONYM(S)

ONR

11. SPONSOR/MONITOR'S REPORT NUMBER(S)

12. DISTRIBUTION/AVAILABILITY STATEMENT

Approved for Public Release; distribution is Unlimited

13. SUPPLEMENTARY NOTES

14. ABSTRACT

The technical objectives of this project were to perform shipboard power system performance metric refinements, early-stage assessment computational tool investigation, and the application of these to NGIPS alternative architectures and technologies. Progress towards metric-based optimization approaches to early-stage design exploration is described. The establishment of a notional medium-voltage dc system for use in system studies is discussed. The development of early-stage modeling techniques is described. The results of studies focused on the energy storage sizing and location are included. Finally, an approach for early-stage modeling of power system protection schemes is included.

15. SUBJECT TERMS

Design exploration, energy storage, metric, modeling, simulation

16. SECURITY CLASSIFICATION OF:			17. LIMITATION OF ABSTRACT	18. NUMBER OF PAGES	19a. NAME OF RESPONSIBLE PERSON
a. REPORT	b. ABSTRACT	c. THIS PAGE			
U	U	U	UU	40	19b. TELEPHONE NUMBER (Include area code)

NGIPS Early Design Space Assessment

Award No: N00014-12-1-0426

Final Technical Report

Aaron M. Cramer

University of Kentucky

20140728310

Table of Contents

List of Figures

Introduction

Adaptation, refinement, and extension of prior highly successful ONR-funded early-stage design space exploration methods and tools were pursued in support of the Navy's Next Generation Integrated Power Systems (NGIPS) transition to an electric naval force. This investigation built on prior work in collaboration with and in support of Electric Ship Research and Development Consortium (ESRDC) NGIPS architecture studies. Original proof-of-concept demonstration of the proposed simulation-based design optimization approach was accomplished under the ONR-funded Integrated Reconfigurable Intelligent System (IRIS) project. The primary objective of the concluded effort was to transition these design methods, metrics, and tools to the representative NGIPS systems under development by ESRDC. The prior work validated the approach using a modular notional set of electro-mechanical-thermal-fluid ship system models. In addition, the prior work provides important insights for improving early design space methods, metrics, and tools. In the concluded effort, the PI's experience with modeling, simulation, optimization, and design space exploration contributed to ESRDC efforts, using input from the larger research community to lead to refined methods and metrics for quantitative assessment of system architectures. Existing computational tools were extended for the quantitative assessment of representative NGIPS systems.

The ability to make early design phase quantitative comparisons between alternative NGIPS architectures and technologies is essential to guide electric naval force from research to reality. Early quantitative assessment can reduce the required design time by eliminating unpromising design alternatives earlier in the design cycle. Early design space exploration can also focus research and development investments toward the technologies that are most likely to have significant ship impact. The concluded effort addressed methods, metrics, and tools for early-stage design exploration that are essential for the successful development and fleet introduction of NGIPS. Quantitative assessment using appropriate metrics and representative ship technical architectures establishes the relative advantages of various competing technologies within the NGIPS Roadmap. Furthermore performance with respect to various design reference missions, concepts of operation, control strategies, and threat scenarios can be assessed quantitatively.

The PI's dissertation research provided a proof-of-concept demonstration under the ONR IRIS project. This prior effort performed proof-of-concept early design space exploration and established the modular layered approach to the modeling and simulation of complex dynamically interdependent systems shown in Figure 1. The efficacy of this modular approach to managing the simulation model complexity was confirmed using the notional electric warship integrated engineering plant shown in Figure 2. This work was expanded and improved in the concluded effort as described below.
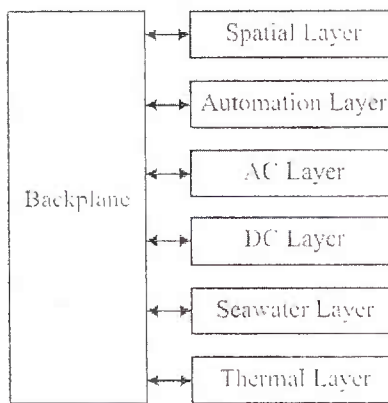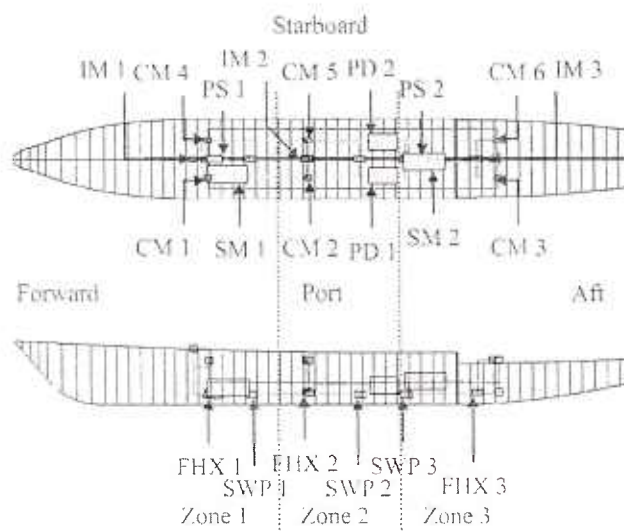
Figure 1. Layered Simulation Approach

Figure 2. Notional Integrated Engineering Plant

Technical Objectives and Approach

The technical objectives of this project were to perform shipboard power system performance metric refinements, early-stage assessment computational tool investigation, and the application of these to NGIPS alternative architectures and technologies. Towards the technical objectives described above, the four tasks described below were pursued in this effort. The first task is to study/refine metrics for measuring shipboard power system performance. In order to make quantitative comparisons between various power system architectures, it is necessary to have sufficient metrics to assess the performance of a power system. The metrics should span operational modes (peacetime through damage control) and describe both the expected performance of the system in these situations and the risk of unacceptable performance.

In previous work, operability has been used as a measure of warship power system performance during a hostile disruption. Operability represents a weighted, time-varying measure of how well the power system delivers power to loads following a disruptive event. The key feature of operability is that it is load centric: it is calculated based on continuity of service to loads. However, the previous treatment of operability did not include the sensitivity of loads to outages of varying durations. Operability, if appropriately refined, can provide the basis for assessing power system performance following both survivability- and reliability-related events.

For power system performance during normal conditions, efficiency provides a meaningful measure. However, like a security-constrained economic dispatch problem in terrestrial power systems, the warship power system is unlikely to be operated in a maximum efficiency mode without regard for the effects of a reliability-related fault in the system. Reliability may be assessed by consideration of the failure rates of the various components in the system and the impact of their failure on system operability. For example, the reliability of a power system could be described in terms of the mean time to a given operability degradation.

The PI has previously proposed system dependability as a measure of power system performance over a set of hostile disruptions. In particular, average system dependability was proposed as the mean operability over a set of hostile disruptions. It represents the average system performance under disruptive conditions. Similarly, minimum system dependability was proposed as the minimum operability over the set of disruptive conditions. Together, these two metric represent the expected performance and a measure of risk. A well designed system would seek to maximize the combination of those two metrics. However, minimum system dependability is fairly difficult to assess (particularly in system optimization studies). Also, as a risk metric, it is fairly conservative (because it only considers the absolute worst possibility). It is possible that other risk metrics, like variance, value-at-risk, and expected shortfall, may be both easier to evaluate accurately and more consistent with the risk preferences of decision makers.

Ultimately, a relatively small number of quantitatively evaluable metrics are required for evaluating shipboard power system performance over the range of conditions in which the system must operate. These metrics can be used to make objective comparisons between competing system designs. The PI collaborated with the United States Naval Academy, other ESRDC institutions, and NSWC to establish representative missions, threats, damage scenarios, and metrics by which to evaluate designs at an early stage.

The second task is to investigate computational tools for early-stage assessment. The aging sampled genetic algorithm has been previously developed by the PI to solve minimax optimization problems. This type of problem is encountered when one wishes to find a system design with the best possible worst-case behavior. This algorithm was adapted to solve minimean problems in which the system design with the best expected behavior is sought. These two

algorithms represent attempts to maximize separately the worst-case and average behaviors. In practice, a system design that simultaneously has high expected performance and low risk of bad performance may be sought. Computational tools that can facilitate this type of early-stage assessment were investigated.

The third task is to apply the metrics to a notional power system. The metrics described above were demonstrated by calculating their values for a notional power system design. In particular, a notional MVDC system was chosen based on the ESRDC baseline systems, a simulation model of the system was developed, and the metrics were calculated for this system. This has provided an opportunity for early feedback regarding the nature of the metrics. In particular, if the metrics predict values that do not correspond with decision makers expectations for what constitutes a good power system design, they will provide a data point around which stakeholder feedback can be articulated and incorporated into metric specification. This is used as a basis for pursuing the fourth task, to study dependability metrics for measuring shipboard power system performance.

Technical Progress

The PI made progress on the study and refinement of metrics for shipboard power system performance. Characteristics of the required metrics within the context of early-stage design have been identified. It has been argued that the early design space should be carefully identified to focus the selection process on key architectural and technological decisions. Traditional metrics such as mass and efficiency remain very relevant measures of system performance, but these metrics can be complemented with system metrics that quantify the dynamic performance of the system subjected to large load transients, faults, failures, and combat-induced battle damage. Based on prior work, an integrated engineering plant (IEP) can be viewed as a service provider. From this perspective, dependability metrics can be used to assess the IEP's ability to continue to provide the continuity of vital services in support of the ship offensive and defensive mission objectives. Roughly speaking, a dependable IEP must be agile and resilient. The use of a metamodeling framework was proposed to reduce the complexity of the system parameterization while permitting the evaluation of dynamic system performance metrics. For each major component within the system, a set of component-level metrics can be defined that allow for tradeoffs in component design to be understood in terms of system impact. In this way, component design can be considered as motion along a Pareto-optimal front, reducing the complexity of the component representation in the system model. The PI contributed to a paper presented at the ESRDC 10th Anniversary Meeting on quantification of vulnerability in early-stage ship design that presented a view of this approach. The PI participated in a Metrics Workshop in Philadelphia in September 2012 to further refine the metrics used to measure shipboard power system performance. At this workshop, the dependability metrics that have been proposed and refined by the PI were identified as candidate metrics for early-stage assessment, and the PI has continued to investigate alternative risk metrics as shown in Figure 3 and in the energy storage study described below.
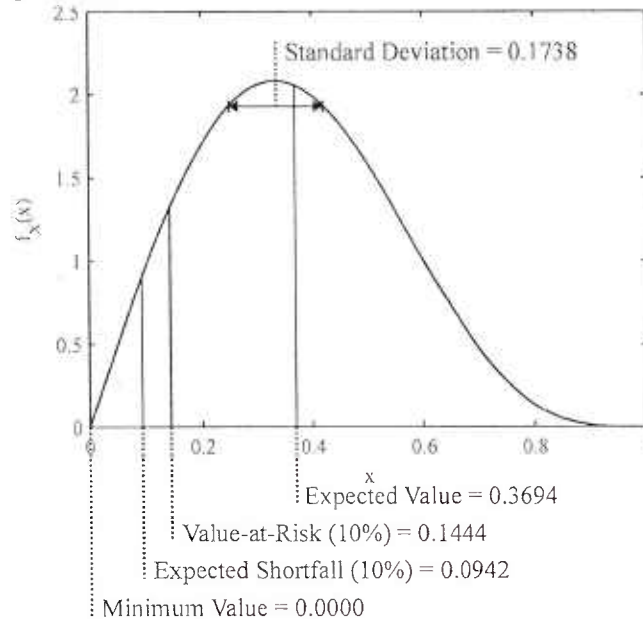

Figure 3. Alternative Risk Measures

5

The PI also conducted an initial investigation into the feasibility of developing advanced optimization-based approaches to early-stage design space exploration. In particular, the PI considered how to extend the aging sampled genetic algorithm shown in Figure 4 to improve the efficiency of optimization methods involving stochastic behavior. In particular, when considering a distribution of possible disruptions, it becomes important to understand how a system design will behave against the set of possible disruptions. The first method that was considered is the use of adaptive sampling to use function evaluations more efficiently. In this method, estimates of the overall system performance are constructed by evaluation of the system performance over a sample. Candidate systems are compared and a probability that one system is actually better than another is estimated. When the probabilities show that potentially good solutions are indeterminate from each other, additional sampling is applied to those solutions. This allows expensive function evaluations to be used only for solutions in which doubt remains with respect to their relative quality. An example showing the probability estimation is shown in Figure 5. The second method to perform system-level design exploration is the generalization to the aging sampled genetic algorithm to perform multiobjective optimization. In stochastic problems, the relationship between risk and reward is important to decision makers. In previous work, the maximum reward and minimum risk points were identified for a given design as shown in Figure 6. By generalization of the aging sampled genetic algorithm, the entire curve representing the tradeoff between risk and reward can be estimated.
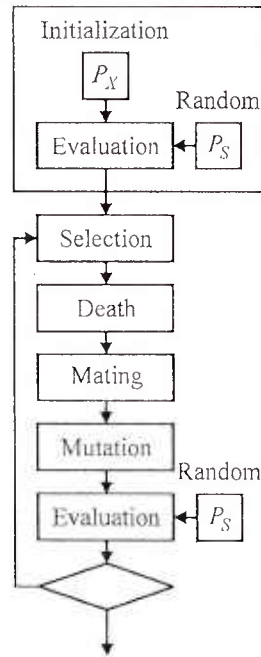

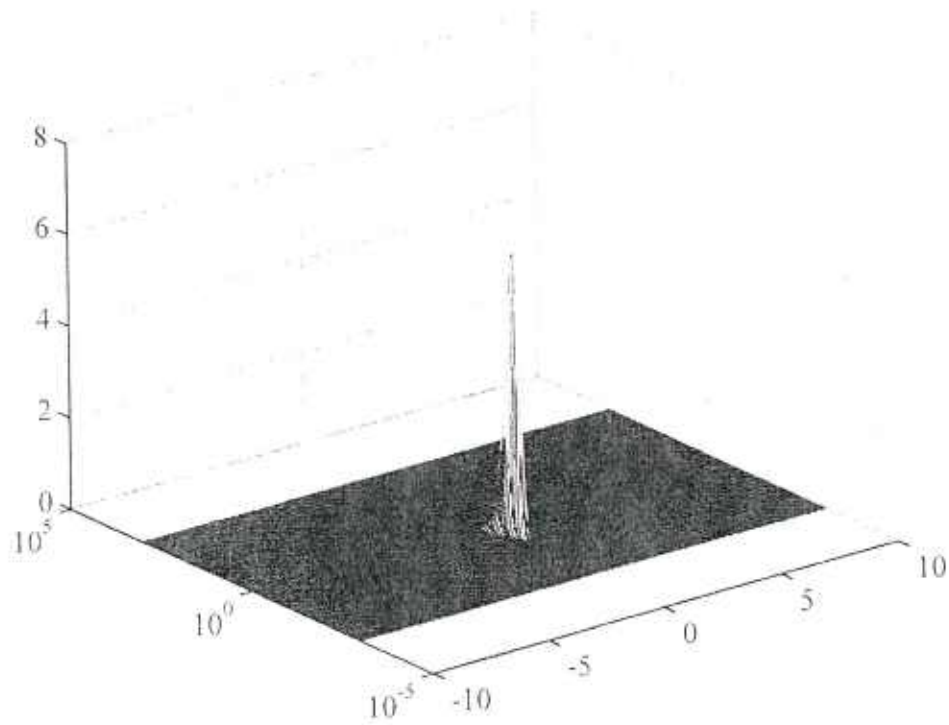Figure 4. Aging Sampled Genetic Algorithm
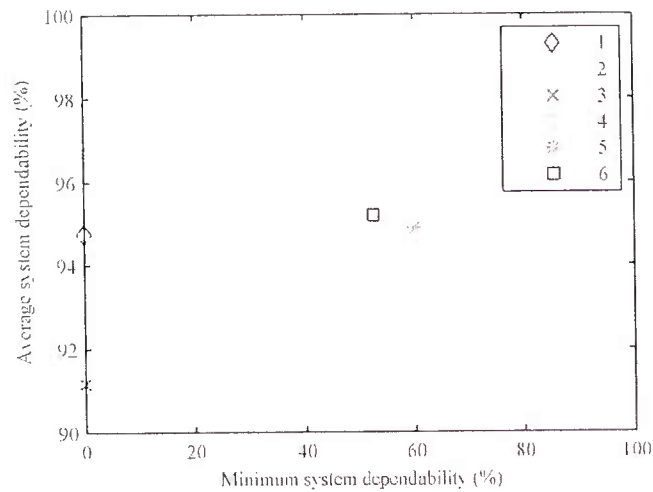
Figure 5. Sample Probability Density Estimate

Figure 6. Reward Versus Risk Optimization

The PI worked with the United States Naval Academy and the Massachusetts Institute of Technology to develop an appropriate representation of the ESRDC notional MVDC system. A combined spatial-electrical simulation model of this system was constructed and was used for

7.

illustration in the studies described below. The electrical structure of the notional MVDC system is shown in Figure 7, and the physical arrangement of the system is shown in Figure 8.
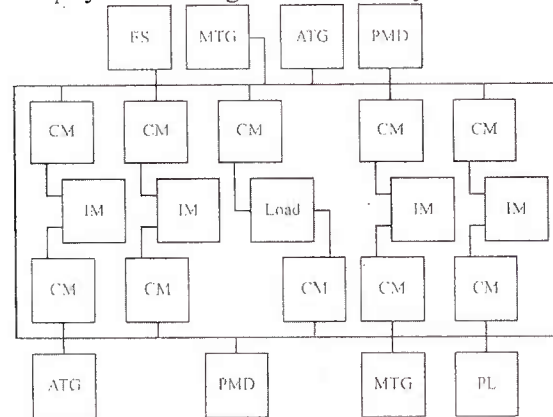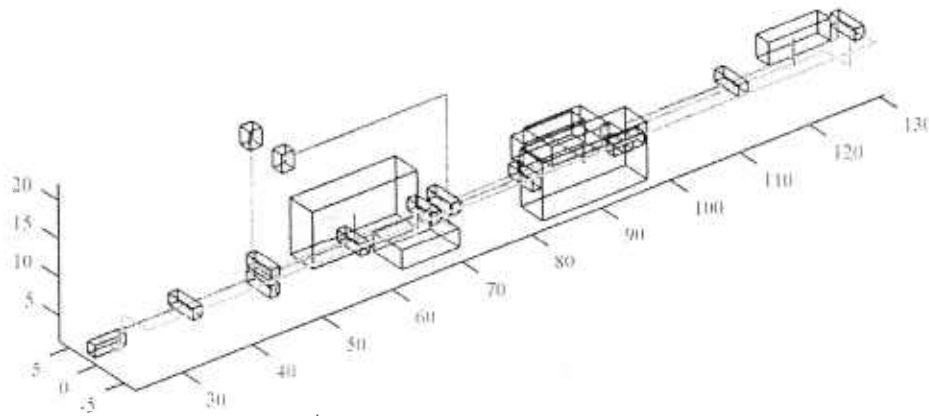

Figure 7. Notional MVDC System

Figure 8. Notional MVDC System Arrangement

The PI has developed an improved method of simulating shipboard electrical systems during the early design stage. Neglect of electrical dynamics has proven very useful for early-stage design space exploration. However, two significant shortcomings associated with previous methods for modeling power systems in this manner were identified. These shortcomings pose significant difficulties for the use of this technique for larger scale systems. A linear programming approach that alleviates these problems was proposed and demonstrated in several system studies. It is shown that the results of this method correspond with those obtained using the previous method, but that the proposed method is nearly 600 times faster than the existing method. This speedup is significant and allows the simulation method to be used for early stage design exploration. The improved method is described in the paper "Shipboard electrical system modeling for early-stage design space exploration," which is included in Appendix 1 and was presented at the IEEE Electric Ship Technologies Symposium 2013.

In response to a Navy white paper, two studies showing the influence of energy storage decisions on an MVDC shipboard power system were performed using the proposed simulation method. These studies pursue the questions posed in the white paper. In particular, the first study

assesses the effect of energy storage amount on the performance of the mission loads and the volume of the power system. The second study assesses the effect of centralizing energy storage. Both of these studies were performed using the modeling approach and notional MVDC system described above. Monte Carlo simulation was performed to show the effect of various levels and locations of energy storage capability on mission performance. This data was used to calculate expected performance, risk, and volume measures. The report on these studies is included in Appendix 2.

Finally, the PI proposed a method for extending early-stage modeling methods to consider nonideal circuit protection behavior. The method generalized the existing approach to consider the effect of the behavior of breakers and sectionalizers on the ability of the power system to provide power through both accidental faults and those resulting from damage. This entailed modifications to the bus model to account for nonideal sectionalizing behavior and modifications to the generator model to address temporary generator bus faults. This approach was demonstrated using the notional power system shown in Figure 7. This work is described in the paper "Modeling and simulation for early-stage quantitative assessment of medium-voltage dc power system protection schemes," which is included in Appendix 3 and was presented at the ASNE Electric Machines Technology Symposium 2014.

Appendix 1

A. M. Cramer, H. Chen, and E. L. Zivi, "Shipboard electrical system modeling for early-stage design space exploration," in *IEEE Electric Ship Technologies Symp., 2013*, Arlington, VA, pp. 128–134, 22–24 Apr. 2013.

Shipboard Electrical System Modeling for Early-Stage Design Space Exploration

Aaron M. Cramer, Hanling Chen
Department of Electrical and Computer Engineering
University of Kentucky
Lexington, KY, USA
Email: cramer@engr.uky.edu, hanling.chen@uky.edu

Edwin L. Zivi
Weapons and Systems Engineering Department
United States Naval Academy
Annapolis, MD, USA
Email: zivi@usna.edu

Abstract—In early-stage design exploration, it has been found that electrical dynamics do not significantly affect the dependability of an integrated engineering plant. Therefore, it has been found useful to neglect these electrical dynamics and focus on mechanical, thermal, and fluidic dynamics in assessing system performance. Previous methods of accomplishing this goal involve the use of linear programming to describe the behavior of the electrical system. Herein, two significant shortcomings of the existing linear programming methods are identified, and a method of representing the electrical system that addresses these shortcomings is proposed. The proposed method is demonstrated in several system studies.

I. INTRODUCTION

The integrated engineering plant (IEP) of an electric warship can be viewed as a service provider that is responsible for providing services such as electric power and thermal management to the mission loads that it serves [1]–[3]. As such, its performance must be measured with respect to its ability to provide continuity of service to these loads across the variety of scenarios in which it must operate [2], [4]. The desired IEP design should be dependable [5].

The operability metric has previously been defined as a measure of the performance of an IEP during a specific scenario [2]. Dependability metrics have been derived from the operability metric as measures of the IEP performance over the range of scenarios in which the IEP must operate [2]. The assessment and optimization of dependability require a great number of operability evaluations [2], [4]. Furthermore, it has been found that the electrical dynamics of the IEP have little effect on the dependability of the IEP so long as the electrical system has been well designed (e.g., stable) [4], [6]–[8]. Therefore, the computational burden of operability evaluation can be reduced by neglecting the electrical dynamics of the IEP in the IEP system simulation [4], [6]. A previously proposed approach to this has involved the use of linear programming to model the action of the power system [6]. In this approach, the mechanical dynamics associated with prime movers are retained, but the electrical power flow is modeled statically. A linear objective function is maximized in which the weights associated with each load are equal to the weights of the loads in the operability calculation. This objective function is a heuristic approximation of an ideal power management system in which the solution to

the optimal power management problem is approximated by the solution to a static problem at each moment in time. While this approximation is potentially optimistic and does not completely represent the time dependence associated with the power management problem (particularly in the presence of energy storage), it is a useful approximation for early-stage design because it can be evaluated at a stage in the design process when little information about the power management system is available.

Neglect of IEP electrical dynamics has proven very useful for early-stage design space exploration [4], [7]. Herein, two significant shortcomings associated with previous methods for modeling the IEP in this manner are described. These shortcomings pose significant difficulties for the use of this technique for larger scale systems. Herein, a linear programming approach that alleviates these problems is proposed and demonstrated in several system studies. The remainder of this paper is organized as follows. In Section II, two significant shortcomings of the previous linear programming approach described in [6] are described. Then, the proposed linear programming approach is set forth in Section III. Next, the proposed method is demonstrated in Section IV.

II. PREVIOUS METHOD

Two significant shortcomings associated with the previous linear programming approach [6] have been identified and are addressed herein. The first shortcoming is the potential to attempt to solve infeasible linear programs. Due to the finite power slew rates of the prime movers, it is possible that, in the presence of sudden load shedding (e.g., due to disruptive conditions), no solution may be found in which a generators output power will be greater than or equal to its minimum power output. In this case, the generator would overspeed and trip offline. In the previous linear programming approach, such a situation would result in an infeasible linear program, the solver would indicate this, and the offending generator would be deactivated. In the proposed model, the linear program is always feasible. When a generators output must be less than its minimum output, it does so via a heavily penalized slack variable. A zero-crossing function associated with this slack is constructed, and this zero crossing can be located by the simulation solver in order to deactivate the generator. This

avoids the difficulty associated with handling infeasible linear programs; the linear programs are feasible by construction.

The second shortcoming associated with the previous linear programming approach to this problem involves the consideration of load sharing. In normal operation, generators may share power in proportion to their ratings. Similarly, converters might share zonal load, and propulsion drives may share responsibility for the ships thrust. In the previous linear programming approach, consideration of load sharing is performed by considering a large number of sharing cases independently. Each sharing case represents a situation in which one or more devices are explicitly sharing load, setting specific equality constraints on the outputs of these devices. Each case is represented by a separate linear program, and at each time step, each linear program is solved. The solution to the case that has the highest objective function is considered the correct solution. The requirement of solving multiple linear programs is problematic because linear programming is the most time consuming task in such a simulation. Herein, the linear programming approach is improved to require only one linear program solution per time step. This linear program is slightly larger in terms of decision variables. Load sharing is promoted in the cost function of the linear program, and equivalent results to those found in previous approaches are found.

III. LINEAR PROGRAMMING APPROACH

The linear-programming approach to electrical power system modeling involves approximating the behavior of the power system using a static linear program at each time step. Linear programs of the following structure are derived:

$$\max_{\mathbf{x}} \mathbf{c}^\mathrm{T}\mathbf{x}$$
$$\text{subject to } \mathbf{A}\mathbf{x} \leq \mathbf{b}$$
$$\mathbf{A}_{eq}\mathbf{x} = \mathbf{b}_{eq} \qquad (1)$$
$$\mathbf{x} \geq 0.$$

The elements of the vector $\mathbf{x}$ correspond with variables describing the operation of various elements in the power system. These elements and their constraints are described below.

A. Interconnect Model

Each interconnect represents a point at which two buses (a "from" bus and a "to" bus) may be disconnected. The manner of this disconnection (e.g., dc circuit breaker vs. deenergizing the bus and using low-current switches) is not considered at this level of modeling fidelity. It is simply assumes that the interconnects allow power to flow between buses within the power rating of the interconnect as long as each bus is intact. Each interconnect is represented by two variables P_{to} and P_{from}, and the total power flowing from the "from" bus to the "to" bus associated with the interconnect is $P_{to} - P_{from}$. The decomposition of the interconnect power into the difference of two nonnegative powers facilitates the linear-programming

description of the system. Each power is limited such that

$$P_x \leq \begin{cases} P_{max}, & \text{"from" and "to" buses undamaged} \\ 0, & \text{otherwise} \end{cases} \qquad (2)$$

where $x \in \{to, from\}$ and P_{max} is the maximum capacity of the interconnect.

B. Generator Model

Each generator is represented as the generator and a disconnect capable of isolating the generator from the bus to which it is connected (the "to" bus). The generator has instantaneous minimum and maximum power capabilities P_{min} and P_{max} that describe the ramp rate limits associated with the generator. These are discussed below. The output power of the generator is described as the difference of two variables P_{out} and $\hat{P}_{out}$, i.e., the total output power is $P_{out} - \hat{P}_{out}$. This is a deviation from the linear-programming approach described in [6]. Therein, only one variable is used to represent the generator output, but this creates in a situation in which an infeasible linear program can result. In particular, this occurs in the case where the total system load (or the load present in some island) is insufficient for the generator to avoid output less than its P_{min}. When this happens, the generator would overspeed and trip offline. This behavior is modeled herein as well, but in a manner that avoids infeasible linear programs. In particular,

$$P_{out} \leq \begin{cases} P_{max}, & \text{"to" bus undamaged} \\ & \text{and generator operational} \\ 0, & \text{otherwise} \end{cases} \qquad (3)$$

and

$$P_{out} \geq \begin{cases} P_{min}, & \text{"to" bus undamaged} \\ & \text{and generator operational} \\ 0, & \text{otherwise} \end{cases} \qquad (4)$$

describe the upper and lower bounds on the nominal component of the generator output power P_{out}, and

$$\hat{P}_{out} \leq \begin{cases} P_{min}, & \text{"to" bus undamaged} \\ & \text{and generator operational} \\ 0, & \text{otherwise} \end{cases} \qquad (5)$$

allows the total generator output power to fall below P_{min}. This deviation below the minimum power limit is penalized in the objective function (i.e., the vector $\mathbf{c}$), but it allows the linear program to remain feasible. Deviations below the minimum power limit are detected using the zero-crossing-detection functionality of a given ODE solver, and when they are detected, the generator is marked as inoperative. This is actually simpler than the method of detecting this condition in the previous formulation [6]. In this formulation, the condition can only be detected by determining that no linear program for the system is feasible at a point in time. However, the linear-programming solver will generally not indicate which constraint is causing the infeasibility. Therefore, there is not a straightforward approach for determining which generator should trip offline.

The generator is modeled to have a slew rate pP_{slew} at which its power can increase or decrease. This model is based on the generator model described in [6]. Herein, a slew rate of 10%/s is utilized, but different slew rates would be appropriate for different types of generators. In particular, the instantaneous output power P of a generator should lie between P_{min} and P_{max}. These operating limits evolve according to

$$\frac{dP_{min}}{dt} = \text{bound}\left(\frac{P_{min,ss}(P) - P_{min}}{\tau}, -pP_{slew}, pP_{slew}\right) \tag{6}$$

$$\frac{dP_{max}}{dt} = \text{bound}\left(\frac{P_{max,ss}(P) - P_{min}}{\tau}, -pP_{slew}, pP_{slew}\right) \tag{7}$$

where

$$P_{min,ss}(P) = \max\{(1 - \epsilon)(P - P_{max,nl}), 0\} \tag{8}$$

$$P_{max,ss}(P) = \min\{(1 + \epsilon)P + P_{max,nl}, P_{rating}\} \tag{9}$$

and τ is a time constant (set to 1 s) associated with the slew-rate limitation, ϵ is a coefficient (0.05) that describes the range in which the power can change instantaneously, and $P_{max,nl}$ indicates the amount of power that is available instantaneously from no-load conditions (here assumed to be 10% of rated power).

C. Converter Model

A converter represents a generic power conversion device that moves power from one bus (the "from" bus) to another bus (the "to" bus). The converter is represented as capable of isolating faults on either bus from the other. If this assumption does not hold, the method of calculating the status of a given bus can be extended to consider dependence on the status of another bus. The converter is also represented as capable of unidirectional power flow, but bidirectional power flow can be represented by two converters in antiparallel. Each converter has two power variables P_{in} and P_{out}. The output power is limited as follows:

$$P_{out} \leq \begin{cases} P_{rating}, & \text{"from" and "to" buses undamaged} \\ & \text{and converter operational} \\ 0, & \text{otherwise} \end{cases} \tag{10}$$

and the input power is related by the converter's efficiency:

$$P_{in} = P_{out}/\eta. \tag{11}$$

D. Load Model

A load represents a sink for power connected to a bus (the "from" bus). The load power P_{in} is limited by the maximum power of the load (possibly time varying):

$$P_{in} \leq \begin{cases} P_{max}, & \text{"from" bus undamaged} \\ & \text{and load operational} \\ 0, & \text{otherwise.} \end{cases} \tag{12}$$

As the purpose of the power system is to provide power to its loads, the objective function rewards power delivery to each load in proportion to the current weight of that load. These weights are derived from mission requirements and vary with time and mission.

E. Bus Model

For each bus, the total power flowing into the bus must sum to zero. Therefore, for each bus, an equality constraint can be constructed such that

$$\sum P_{in} = 0. \tag{13}$$

This equality constraint can be constructed by consideration of the interconnects that join a bus with neighboring buses. For an interconnect in which the bus in question is the "to" bus, the incoming power is $P_{to} - P_{from}$. For an interconnect in which the bus is the "from" bus, the incoming power is $P_{from} - P_{to}$. For any generator connected to the bus, the incoming power is $P_{out} - \hat{P}_{out}$. For any converter in which the bus in question is the "from" bus, the incoming power is $-P_{in}$, and for any converter in which the bus in question is the "to" bus, the incoming power is P_{out}. For any load connected to the bus, the incoming power is $-P_{in}$. One such equality constraint is constructed for each bus in the system.

F. Load Sharing

The consideration of load sharing is another manner in which the proposed method deviates from that proposed in [6]. In [6], it is noted that there are situations in which generators or converters should share their total load in proportion to their ratings. However, under abnormal operating conditions, a requirement that this happen can result in less total power being delivered to loads. Therefore, sharing scenarios are constructed in [6] that describe every possible combination of components that could be sharing load at a point in time. These scenarios each induce a unique set of additional equality constraints on the output powers of the components governed by them. A linear program is then formulated and solved for each of these scenarios, and the scenario in which the solution is optimal from the point of view of load satisfaction and load sharing is selected. This involves consideration of various sharing groups. The generators are assumed to form one sharing group with the presumption that under normal operation load would be shared by each generator. Sets of converters that are capable of providing power to the same bus are considered sharing groups as well. Unfortunately, the number of sharing scenarios grows rapidly with the number of devices that can share load and with the number of sharing groups in which these devices participate.

Herein, the same challenge is addressed from the standpoint of a single linear program. This program has additional decision variables, but only one linear program needs to be solved at each time step. Each device that can share power is assigned a positive and negative deviation from the ideal power sharing scenario, α and β, respectively. In each sharing group, the devices that are active are determined. For generators, this means that the generator is operational and that its "to" bus is intact. For converters, this means that the converter is

operation and that its "from" and "to" buses are intact. The total rating $P_{rating,total}$ of all operational devices in the group is determined. An equality constraint for each operational device is established such that

$$\frac{P_{total}}{P_{rating,total}} - \frac{P}{P_{rating}} + \alpha - \beta = 0 \qquad (14)$$

where P_{total} is the total power produced by each member of the sharing group, P is the power produced by the given device, and P_{rating} is the rated power of the given device. The factors α and β are (lightly) penalized in the objective function (i.e., the vector c). In this way, the linear program will seek to deliver maximal power to highly weighted loads, but it will seek solutions where load is shared in cases where this can be done without affecting overall load satisfaction.

G. Method Summary

The proposed method will result in a linear program with $2n_i + 2n_g + 2n_c + n_l + 2n_g + 2n_{sgm}$ decision variables where n_i is the number of interconnects, n_g is the number of generators, n_c is the number of converters, n_l is the number of loads, and n_{sgm} is the number of converters that participate in sharing groups (sharing group members). The resulting linear program will have $2n_i + 3n_g + n_c + n_l$ inequality constraints and $n_b + n_c + n_g + n_{sgm}$ equality constraints where n_b is the number of buses. Furthermore, the approach will involve a differential equation describing the generators' power limits with $2n_g$ state variables.

This can be compared with the method in [6] in which multiple linear programs must be solved. Each linear program will have $2n_i + n_g + 2n_c + n_l$ decision variables, which is fewer than the proposed method. Each will have $2n_i + 2n_g + n_c + n_l$ inequality constraints, which is also fewer than the proposed method, and each will have between $n_b + n_c$ and $n_b + n_c + (n_g - 1) + (n_{sgm} - n_{sg})$ equality constraints depending on which sharing scenario is being considered where n_{sg} is the number of sharing groups in which converters can participate. The number of equality constraints for each of these linear programs is also less than those required for the proposed method. However, despite each linear program being smaller in size, a great number of these linear programs must be solved at each time step. In particular, the total number of cases that must be considered is the product of the number of scenarios in which power can be shared in each sharing group. The same differential equation describing the generators' power limits with $2n_g$ state variables is used with this method.

IV. DEMONSTRATION OF PROPOSED METHOD

The proposed method is demonstrated on the Electric Ship Research and Development Consortium notional medium-voltage dc system as described in [8], [9]. A simplified depiction of this system is shown in Fig. 1. Herein, the energy storage and pulsed load are not represented because it is not necessary to demonstrate the relative advantages of the proposed method. These devices can be incorporated in a straightforward manner (e.g., as given in [6]). Likewise, the
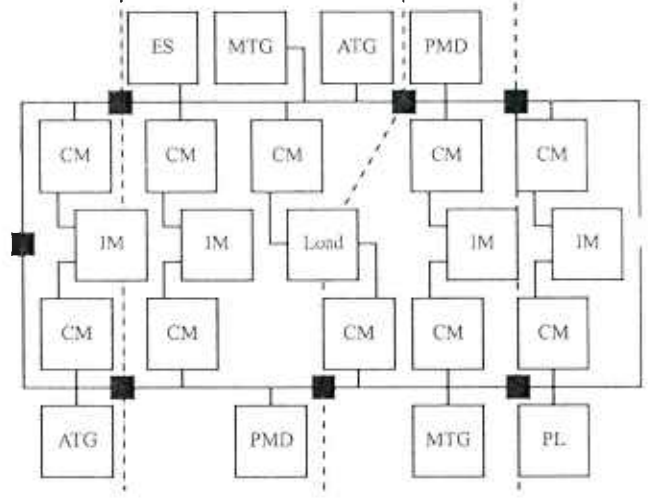

Fig. 1. Notional MVDC system. MTG signifies main generator, ATG signifies auxiliary generator, PMD signifies propulsion drive, CM signifies a dc-dc converter, IM signifies a converter to end-use form, ES signifies energy storage, and PL signifies pulsed load.

TABLE I
SYSTEM SIZE

Parameter	Value
n_i	8
n_g	4
n_c	16
n_l	29
n_b	18
n_{sg}	6
n_{sgm}	12

large load shown in the center of Fig. 1, which represents a radar load, is represented as drawing constant power in steady state. This representation could easily be substituted with an alternative representation without additional difficulty.

In this system, each device resides in one of four electrical zones [10] with interconnects separating the zones. Also, interconnects exist in the forward and aft connections between the port and starboard sides of the system. The pairs of CMs that are aligned vertically are assumed to participate in load sharing. Also, the CMs providing power to the central load are assumed to participate in load sharing. Finally, the two propulsion drives are represented as converters providing power to a fictitious propulsion bus, with various amounts of required propulsion power being represented as loads on this bus. In this sense, the two propulsion drives also participate in load sharing. This system has the sizes shown in Table I.

This system requires a linear program with 117 decision variables, 50 equality constraints, and 73 inequality constraints. The previous linear programming approach discussed in [6] requires 81 decision variables, between 34 and 43 equality constraints, and 69 inequality constraints, but 960 linear programs must be solved per time step. In [6], a
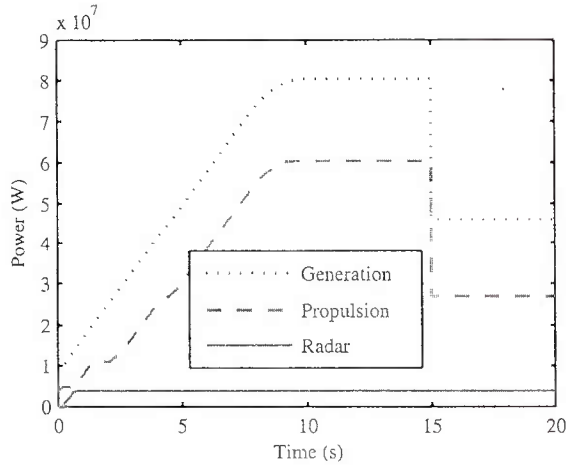
Fig. 2. Simulation results using the previous linear programming method
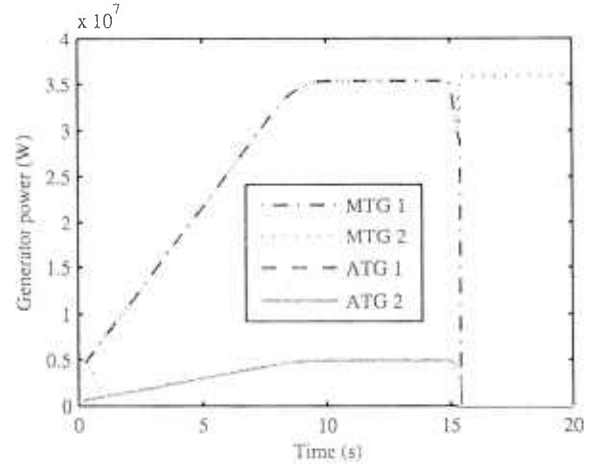

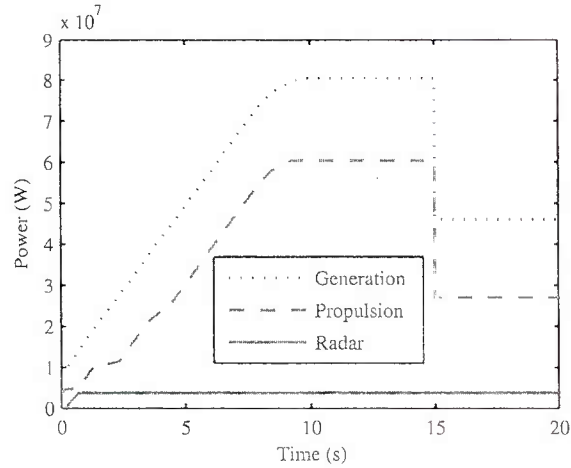Fig. 4. Simulation results of 50% load shed in 1 s

Fig. 3. Simulation results using the proposed linear programming method
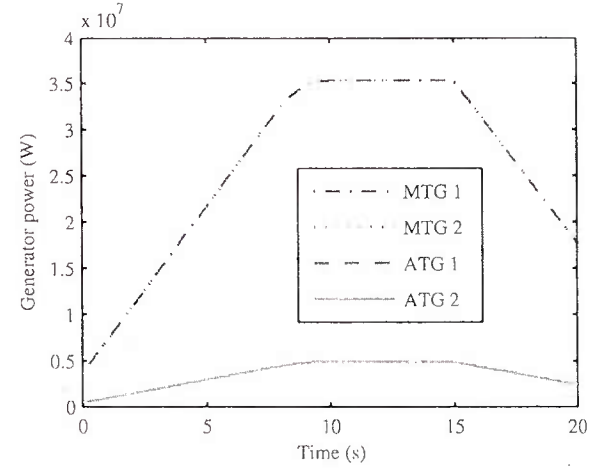

Fig. 5. Simulation results of 50% load shed in 5 s

simulation speed of 15 times faster than real time is reported for a smaller problem. To compare the two approaches, a case in which the system is brought to steady state and at 15 s a generator trips offline is studied. For this study, the loads are weighted in accordance with the weights provided in [8]. MATLAB's ode23tb solver [11] is used to integrate the differential equations and the lp_solve package [12] is used to solve the linear programs (this package was found to solve these linear programs in significantly less time than MATLAB's linear programming solver). The results of simulating the previous method are shown in Fig. 2. The results of simulating the proposed method are shown in Fig. 3. It can be seen that the two methods predict essentially identical system behavior. However, the previous method required 603 s to perform this 20-s study on an Intel Core i7 2.8-GHz processor with 4 GB of memory. On the same computer, the proposed method required only 1.01 s. The excessive computational cost associated with the previous method effectively precludes its use for early-stage design exploration for larger systems.

In another case that demonstrates the ability of the proposed method to detect generator overspeed conditions, the total system load is ramped from 100% to 50% over 1 s beginning at 15 s. The output power of each generator is shown in Fig. 4. This study required 1.30 s to simulate. It can be seen that this sudden load shedding causes both auxiliary generators and one of the main generators to trip offline. This behavior may be slightly unexpected as the auxiliary generators would probably have higher power ramp rate capabilities, but herein, the generators all have common ramp rate limitations. A more gradual load shedding scenario is shown in Fig. 5. In this case, the total system load is shed over 5 s, and this study required 0.99 s to simulate. In this simulation, no generators tripped offline because the load shedding could be handled within the ramp rate limits of the generators.

A final case that is considered is that of a bus fault occuring at the bus where the port main and auxiliary generators are connected. This simulation study lasts 1800 s. At 900 s, the fault occurs, and at 960 s, the system establishes new load
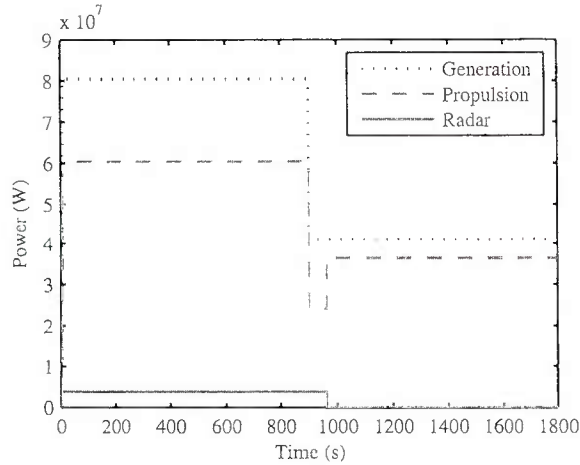
Fig. 6. Simulation results of bus fault followed by change in load weighting

Fig. 7. Simulation results of bus fault followed by change in load weighting with interconnects deactivated

weightings in order to meet mission objectives. In particular, the weight of the propulsion load is promoted to exceed the weight of the radar load. The results of this study are shown in Fig. 6. It can be seen that the total generator power is reduced because the two generators trip offline. Also. the propulsion power is reduced, but the radar power maintains its value due to the weighting of the loads. When the load weights are updated at 960 s to emphasize propulsion, power shifts from the radar and other loads to propulsion.

A similar example is shown in Fig. 7. In this simulation, the interconnects between the port and starboard are deactivated. It can be seen that the generation and propulsion powers are reduced. However, when the system is reconfigured, power is not shifted from the radar load to propulsion. Instead, the propulsion load increases only slightly due to power being shifted from other loads. At this level, the total propulsion power is equal to the rated power of one of the propulsion drives. The other propulsion drive is inoperable because power cannot be delivered to it with the buses split in this manner. A comparison of the resulting ship speed is shown in Fig. 8. It can be seen that the case with the interconnects deactivated actually provides more speed during the 60 s following the fault. However, during this time, the load weightings are such that power would be better spent elsewhere in the system. Following the change in load weighting, the system with the interconnects active provides more speed.

V. CONCLUSION

A previously proposed approach to model the power system has involved the use of linear programming. Two significant shortcomings associated with the previous linear programming approach have been identified. The first shortcoming is the potential to attempt to solve infeasible linear programs. The second shortcoming associated with the previous linear programming approach to this problem involves the consideration of load sharing. An improved method of modeling the shipboard electrical system for early-stage design space ex-
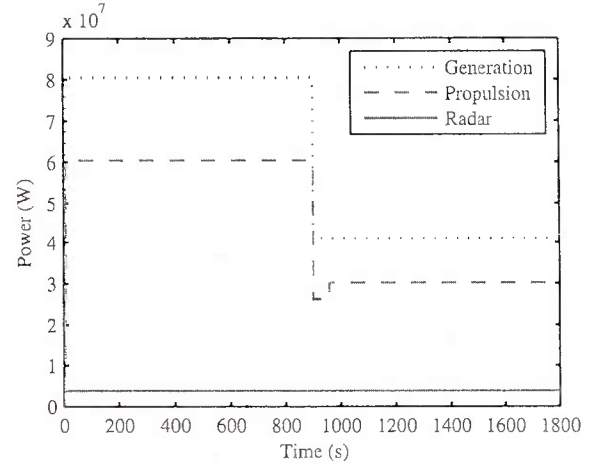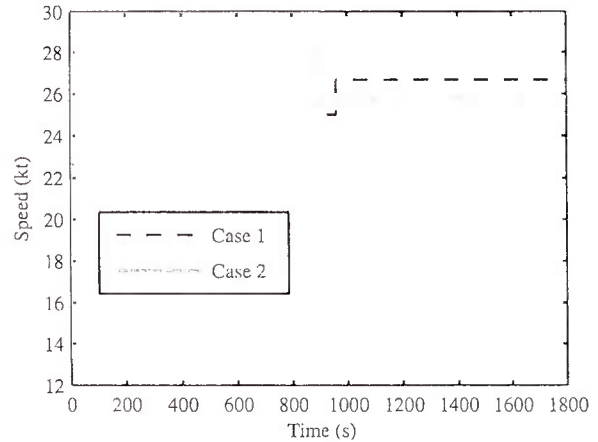

Fig. 8. Simulation results of ship speed following bus fault and change in load weighting. Case 1 represents interconnect active. Case 2 represents interconnects deactivated.

ploration is proposed herein. The proposed method addresses both of these shortcomings and has been demonstrated on a notional medium voltage dc system, allowing the method to be used in early-stage design space exploration studies.

ACKNOWLEDGMENT

REFERENCES

[1] J. P. Walks and J. F. Mearman, "Integrated engineering plant," presented at the Amer. Soc. Naval Engineers Reconfiguration Survivability Symp. 2005, Atlantic Beach, FL.

[2] A. M. Cramer, S. D. Sudhoff, and E. L. Zivi, "Performance metrics for electric warship integrated engineering plant battle damage response," IEEE Trans. Aerosp. Electron. Syst., vol. 47, no. 1, pp. 634–646, Jan. 2011.

[3] M. G. Richards, D. E. Hastings, D. H. Rhodes, and A. L. Weigel, "Defining survivability for engineering systems," in Proc. 5th Annu. Conf. Syst. Eng. Res., 2007.

[4] A. M. Cramer, S. D. Sudhoff, and E. L. Zivi, "Metric optimization-based design of systems subject to hostile disruptions," *IEEE Trans. Syst., Man, Cybern. A, Syst., Humans*, vol. 41, no. 5, pp. 989–1000, Sept. 2011.

[5] E. Zivi, "Design of robust shipboard power automation systems," *Annu. Rev. Control*, vol. 29, no. 2, pp. 261–272, 2005.

[6] R. R. Chan, S. D. Sudhoff, Y. Lee, and E. L. Zivi, "A linear programming approach to shipboard electrical system modeling," in *IEEE Electric Ship Technologies Symp., 2009*, Baltimore, MD, pp. 261–269.

[7] R. R. Chan, S. D. Sudhoff, and E. L. Zivi, "An approach to optimally allocate energy storage in naval electric ships," in *2011 IEEE Electric Ship Technologies Symp.*, Alexandria, VA, pp. 402–405.

[8] J. S. Chalfant and C. Chryssostomidis, "Analysis of various all-electric-ship electrical distribution system topologies," in *2011 IEEE Electric Ship Technologies Symp.*, Alexandria, VA, pp. 72–77.

[9] J. S. Chalfant, C. Chryssostomidis, and M. G. Angle, "Study of parallel ac and dc electrical distribution in the all-electric ship," in *Proc. Grand Challenges Modeling Simulation*, Ottawa, Canada, 2010.

[10] N. Doerry, "Zonal ship design," *Nav. Eng. J.*, vol. 118, no. 1, pp. 39–53, Jan. 2006.

[11] "MATLAB R2012b," The MathWorks Inc.

[12] "lp_solve 5.5.2." [Online]. Available: http://lpsolve.sourceforge.net/

Appendix 2

A. M. Cramer, "Early-stage study of energy storage sizing and location," August 2013.

Early-Stage Study of Energy Storage Sizing and Location

Aaron M. Cramer, University of Kentucky

In response to a white paper [1], two studies showing the influence of energy storage decisions on a medium-voltage dc (MVDC) shipboard power system are described below. These studies pursue the questions posed in the white paper. In particular, the first study assesses the effect of energy storage amount has on the performance of the mission loads and the volume of the power system. The second study assesses the effect of centralizing energy storage.

Baseline System

A baseline system based on the notional MVDC system developed by the Electric Ship Research and Development Consortium is used herein [2], [3]. A simplified depiction of this system is shown in Fig. 1. The arrangement of the system is depicted in Fig. 2. The baseline loads are listed in Table I. The pulsed load depicted in the figure and the table is not utilized herein; instead, several of the zonal loads are replaced with higher-power, short-duration loads. In particular, zone 2 load 3 is replaced with a 5.67-MW load, zone 3 load 3 is replaced with a 7.70-MW load, and zone 4 load 3 is replaced with a 7.09-MW load. These substitutions are intended to represent high-power mission loads with relatively low duty cycles (approximately 5 minutes on and 25 minutes off). In order to service these loads, the baseline system has distributed energy storage modules located in zones 2–4 having capacities of 1.89 GJ, 2.57 GJ, and 2.36 GJ, respectively. In order to account for power elasticity of these mission loads, a time-domain metric is defined as follows:

$$\frac{dv}{dt} = \frac{\max\{p-v, 0\}}{\tau}, \; v(0) = 0 \tag{1}$$

where p is the normalized power flowing into the load (actual power divided by rated power), τ is a time constant that describes how long the mission load requires power in order to perform its mission. This metric takes values on $[0,1]$ and asymptotically approaches the normalized power as it is applied for a sufficiently long period of time. This metric has suitable properties for the study at hand, but variations of this metric or alternative metrics are possible. The value of τ is selected as 65.14 s such that rated power for 300 s will correspond to a performance of 0.99. The values of this performance metric for varying normalized powers and durations are shown in Fig. 3.
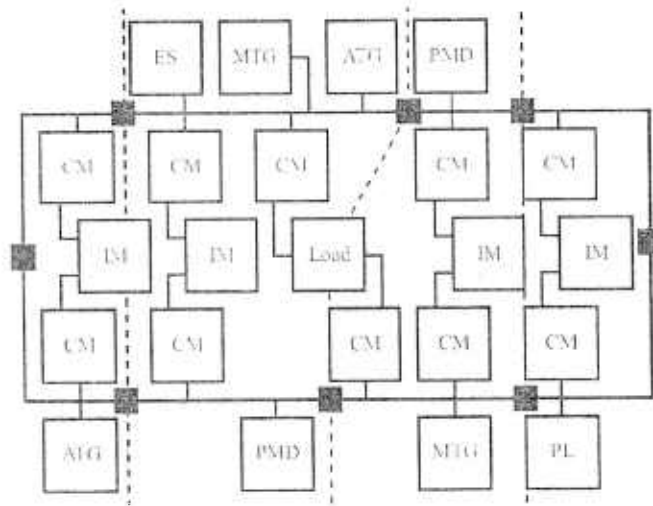
Fig. 1. Notional MVDC system. MTG signifies main generator, ATG signifies auxiliary generator, PMD signifies propulsion drive, CM signifies a dc-dc converter, IM signifies a converter to end-use form, ES signifies centralized energy storage, and PL signifies pulsed load.
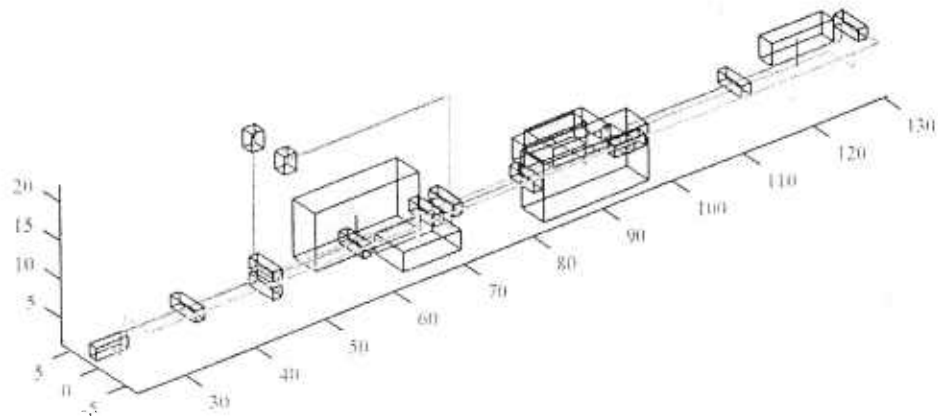

Fig. 2. Arrangement of notional system.

TABLE I
BASELINE SYSTEM LOADS

| Zone	Num	Type	Vital	Cruise (kW)	Battle (kW)	Notes
1	1	DC	V	70	150	Constant impedance resistive
1	2	DC	V	0	135	Constant impedance resistive
1	3	AC	V	840	715	Constant impedance resistive
1	4	AC	V	390	410	450 Vac 3-phase resistive
1	5	AC	NV	275	410	450 Vac 3-phase constant impedance
1	6	AC	NV	7	0	120/208 AC load constant impedance
2	1	DC	NV	0	-	Lumped DC resistive
2	2	DC	V	20	75	Constant impedance resistive
2	3	AC	V	430	1400	Constant impedance resistive
2	4	AC	V	300	750	450 Vac 3-phase resistive
2	5	AC	NV	400	975	450 Vac 3 phase constant impedance
2	6	AC	NV	35	40	120/208 AC load constant impedance
3	1	DC	V	20	40	Constant impedance resistive
3	2	AC	V	1200	1200	Constant impedance resistive
3	3	AC	V	560	1900	Constant impedance resistive
3	4	AC	NV	375	750	450 Vac 3 phase resistive
3	5	AC	NV	4	0	450 Vac 3-phase constant impedance
4	1	DC	V	0	80	Constant impedance resistive
4	2	AC	V	200	480	Constant impedance resistive
4	3	AC	V	415	1750	450 Vac 3 phase resistive
4	4	AC	NV	220	675	450 Vac 3 phase constant impedance
4	5	AC	NV	4	0	120/208 AC constant impedance
Radar		DC	V	2850	3750	DC constant impedance
Pulse		DC	V	0	10000	
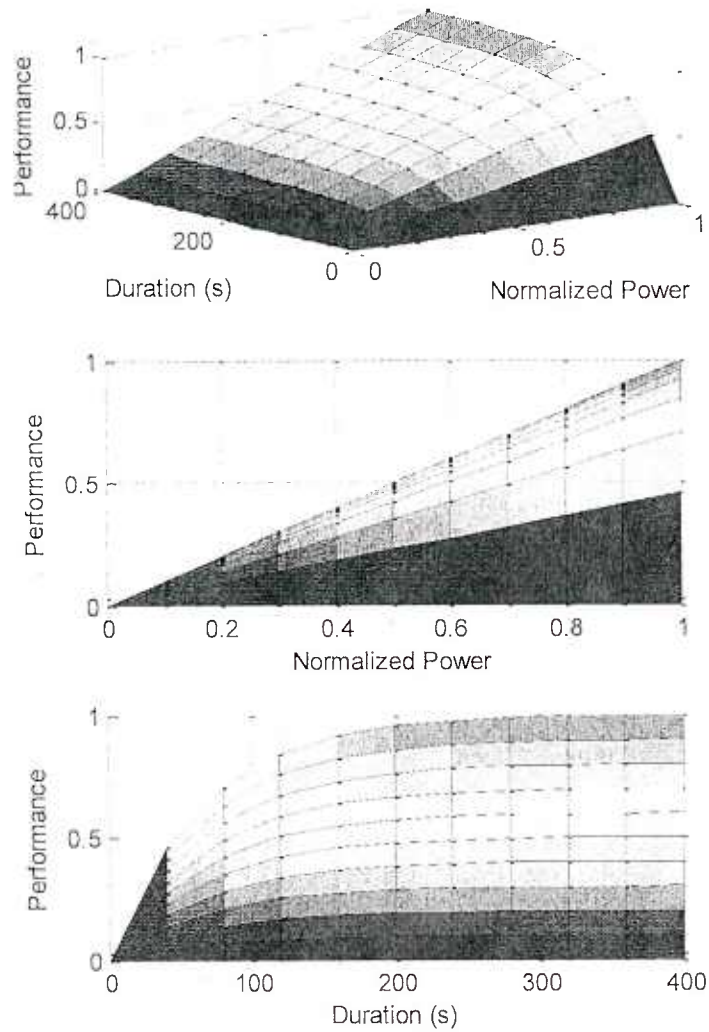
Fig. 3. Performance metric illustration.

Event Space

To consider the performance of such a system with the mission loads described above, the following situation is considered. The system is initially assumed to be at steady state. At 15 s, a disruption occurs. The disruption is modeled as a spherical region of disruption with radius 10.4 m [2]. The centroid of the disrupted region is assumed to be uniformly distributed throughout the volume of the ship. Consideration of alternative distributions is possible. For example, it is possible to consider a distribution of disruptions that is normally distributed on the longitudinal axis. At 30 s, one of three missions (each equally probable and requiring one of the mission loads) is attempted. The mission metric described above is calculated over the following 390 s. The system is simulated using the approach described in [4]. Monte Carlo simulation is performed using 1000 trials. The distribution of mission performance for the baseline system is

shown in Fig. 4. It can be observed that in approximately 12% of the trials the disruption affects the mission load directly, preventing it from being available for the mission. In the remaining trials, the mission is performed effectively because the load relies on local energy storage rather than the power system to perform the mission. A small plateau can be seen in Fig. 4 between approximately 12% and 36%. In these 24% of cases, the local energy storage is sufficient to perform the mission for 300 s, but the power distribution system has been affected by the disruption and cannot augment the energy storage to sustain the load for a longer duration than 300 s.
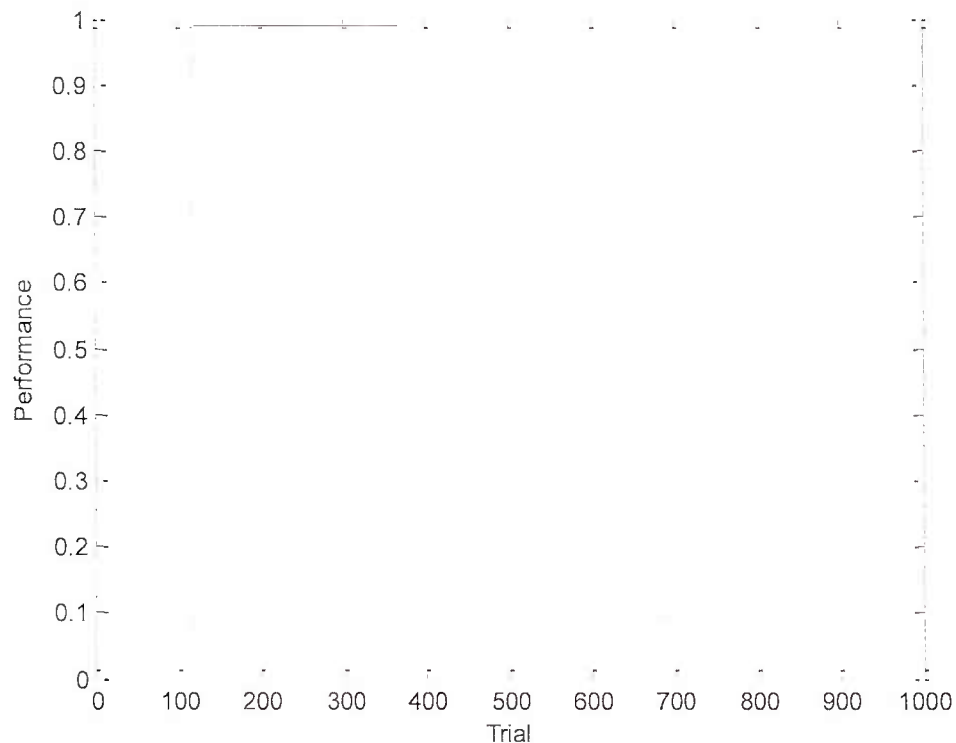

Fig. 4. Baseline system performance.

Herein, two studies are performed. In the first study, the value of various levels of local energy storage capacity is assessed. In the second study, the value of centralizing various levels of energy storage capacity is assessed. In both studies, expected performance, risk, and volume are compared.

Study 1 – Energy Storage Amount

In the first study, the amount of local energy storage available to the loads is varied between 0% and 100% of the values described above for the baseline system. No changes are made to the power ratings of the power conversion equipment in the system because the loads are still intended to be supplied primarily from local energy storage. The results of Monte Carlo simulation are shown in Fig. 5. It can be observed that each system has the same probability of the mission load being unavailable due to disruption. However, as the available energy storage decreases, the mission loads become dependent on the power system to subsidize the energy

provided by the energy storage module. Because the power conversion equipment is not rated to provide peak power to these loads, the power system is limited in its ability to provide this subsidy. This results in lower best-case performance for systems with smaller available energy storage. It also creates a rightward shift in these curves associated with the probability of the power system being affected by the disruption. Some summary statistics associated with these curves are calculated. The mean performance of each of these systems is shown in Fig. 6. In financial risk management, given percentiles of a distribution are used to quantify the risk associated with a distribution, and this metric is called value-at-risk. Various percentiles of the distribution are shown in Fig. 7. The probabilities of unacceptable performance (for given levels of acceptable performance) are shown in Fig. 8. Percentile (or value-at-risk) and probability of unacceptable performance represent alternative ways to quantify risk. With the percentile, a location on the horizontal axis of Fig. 5 is selected, and the performance associated with each system at that location is identified. With the probability of unacceptable performance, a performance on the vertical axis is selected, and the fraction of trials associated with performance below that location is calculated. The choice of risk metric and the parameter associated with that metric (percentile or level of acceptable performance) reflect decision maker risk preferences. Finally, an estimate of volume of each of the systems (energy storage plus power conversion equipment) is shown in Fig. 9. The energy density of the energy storage modules is assumed to be 1.5 GJ/m^3, roughly corresponding to the energy density of lithium-ion batteries. The power density of the power conversion equipment is assumed to be 28 MW/m^3 [5]. It can be seen that the performance (both in terms of expected performance and risk of bad performance) improve with increased energy storage while the volume increases.
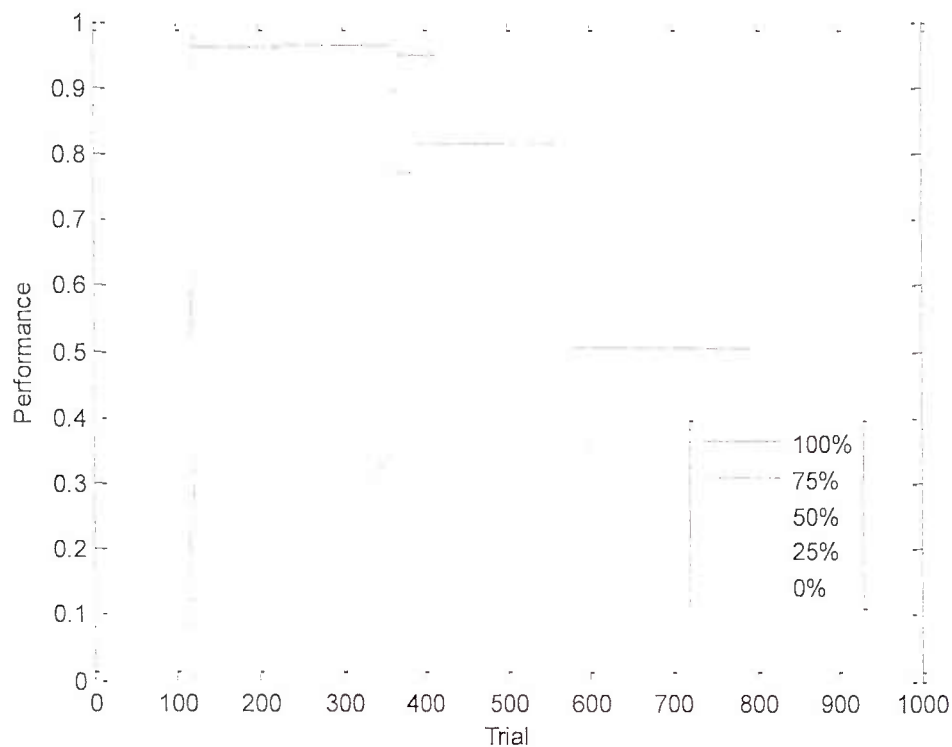
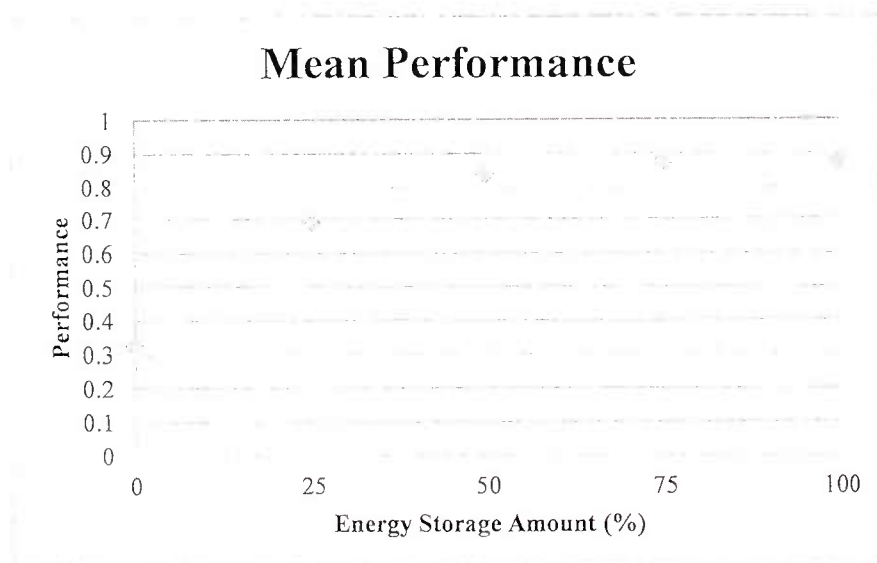

Fig. 5. System performance from study 1.

Mean Performance

Fig. 6. Mean performance from study 1.
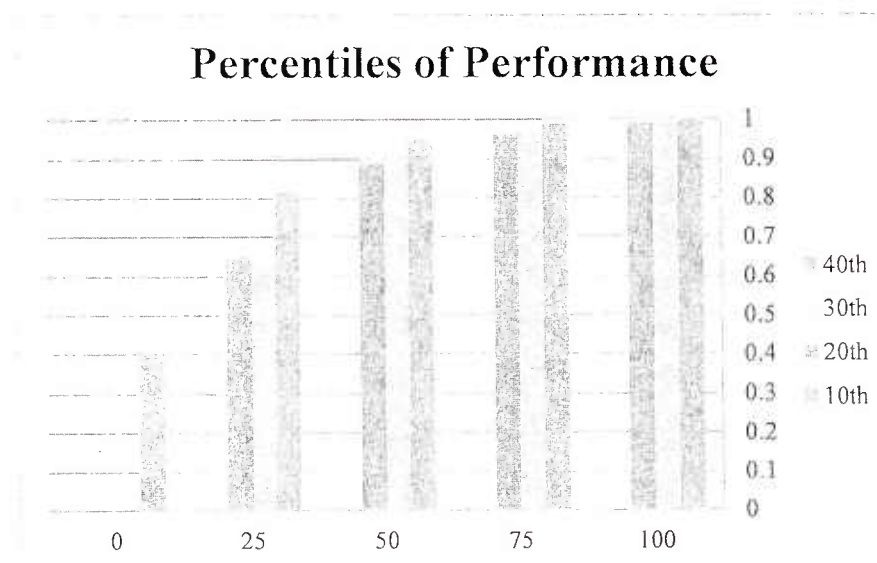
Percentiles of Performance

Fig. 7. Percentiles of performance from study 1.

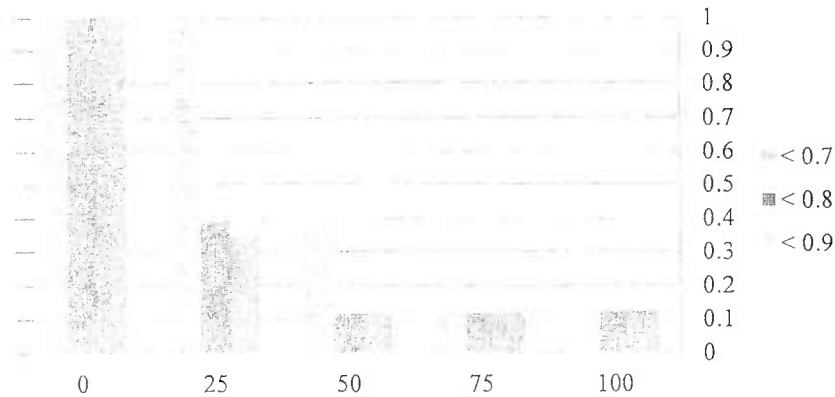## Probability of Unacceptable Performance

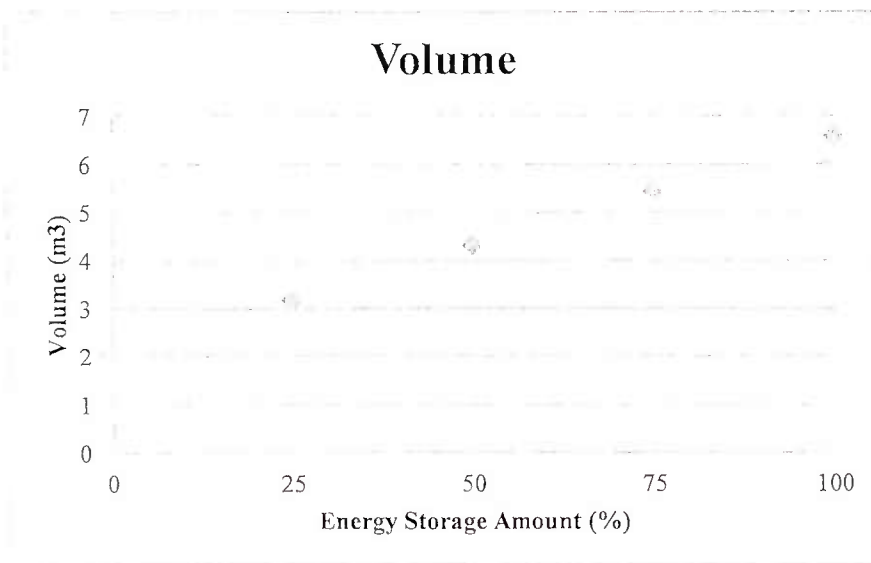Fig. 8. Probability of unacceptable performance from study 1.

Volume

Fig. 9. Volume from study 1.

Study 2 – Energy Storage Location

In the second study, energy storage distribution is varied. Energy storage capacity is moved from the local energy storage modules to the central energy storage module depicted in the upper left corner of Fig. 1. The energy storage distribution is varied from 100% (all distributed) to 0% (all centralized). As energy storage is centralized, the total required energy storage decreases. However, the ratings of the power conversion equipment in the power system must be increased as this equipment will now be responsible for supplying a greater proportion of the peak load of the mission loads. The results of the Monte Carlo simulation for this study are shown in Fig. 10. It can be seen that each system has approximately the same probability of the mission load being unavailable. Then there are a fraction of trials (approximately 15%) in which the centralized energy storage is unavailable. The performance during these trials is limited to

the available distributed energy storage. Thus, the 25% system has a plateau at around 25% performance, the 50% system has a plateau at around 50% performance, and so forth. The mean performance of these systems is shown in Fig. 11. Various percentiles of performance of these systems are shown in Fig. 12. The 25% system shows a worse 30th percentile of performance than the other systems because the choice of 30% roughly corresponds with the edge of the plateau discussed above. By virtue of the samples that were drawn, the 30th percentile of the 25% system falls to the left of the edge while the 30th percentile of the other systems fall to the right of the edge. The probabilities of unacceptable performance (for various levels of acceptable performance) are shown in Fig. 13. It can be seen that the systems with distributed energy storage fractions less than the specified level of bad performance have a higher probability of bad performance than those with a greater level of distributed energy storage. The volume estimates of these systems are shown in Fig. 14. While the volume increases with increased amounts of distributed energy storage, this increase is not as drastic. This is because centralizing energy storage requires greater power ratings of the power conversion equipment to allow them to provide peak power to the mission loads. It is important to note that the second study maintains the same overall energy storage operational capability. This same capability is centralized or distributed to varying degrees. This is different from the first study where the energy storage capability is actually varied in the study. Thus, it would not be appropriate to directly compare Fig. 9 and Fig. 14 for example.
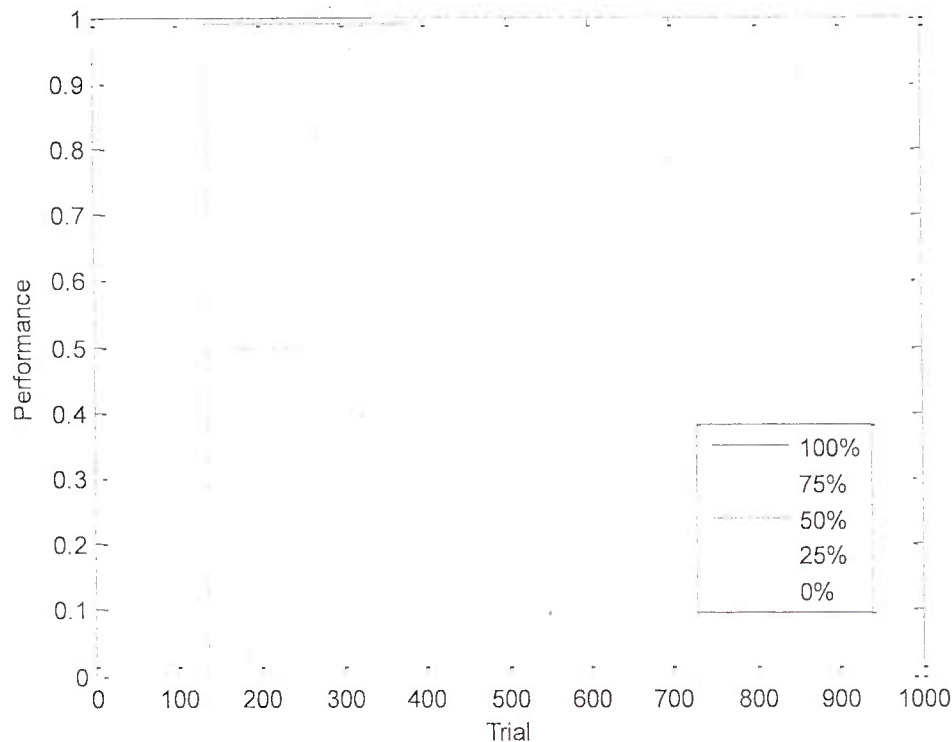

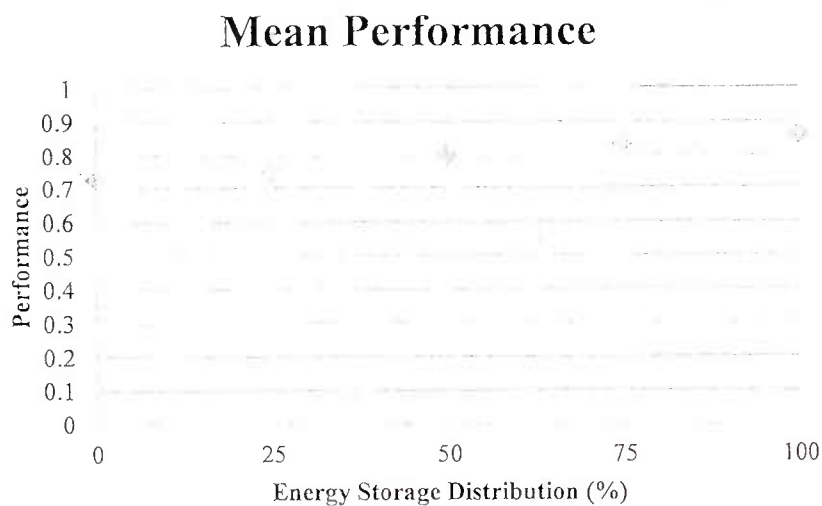Fig. 10. System performance from study 2.

Mean Performance

Fig. 11. Mean performance from study 2.
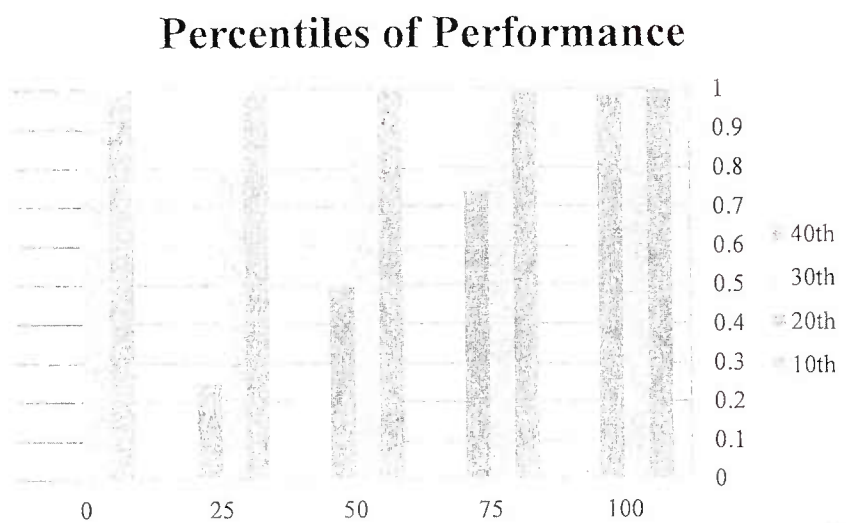
Percentiles of Performance

Fig. 12. Percentiles of performance from study 2.
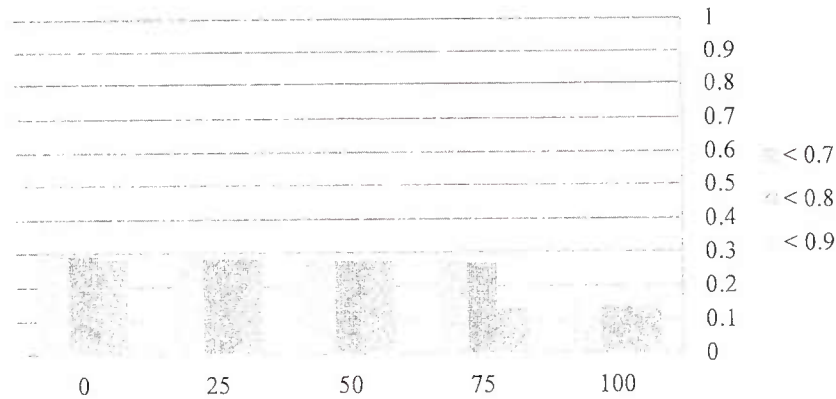
Probability of Unacceptable Performance

Fig. 13. Probability of unacceptable performance from study 2.
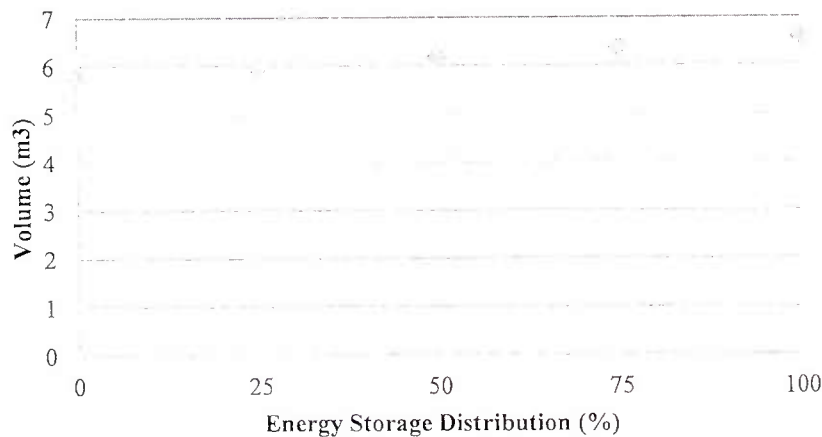
Volume

Fig. 14. Volume from study 2.

Conclusions and Future Work

It has been shown that early-stage modeling and simulation techniques [4] and metric-based approaches (e.g., [6] and [7]) can be used to evaluate early-stage design decisions. Herein, such an approach is used to answer the problems posed in [1], particularly evaluating the impact of both overall energy storage capacity and energy storage location on mission effectiveness. It is found that overall energy storage capacity has a significant impact on mission effectiveness, both in terms of expected performance and risk. Overall energy storage capacity also has a significant impact on power system volume. It is found that distributing energy storage slightly improves expected performance and risk. This also results in a slightly larger power system volume. It is possible that consideration of more mission loads (perhaps with different duty cycles or mission durations) would tilt the volume advantage further in favor of centralizing energy storage

without worsening the centralized energy storage expected performance or risk. In the present study, only three mission loads are considered, and required increases in power conversion capability offset some of the benefits of centralizing the energy storage. Future work suggested by these studies includes:

- Combination of the first and second studies to understand the combined impact of energy storage capacity and location on mission performance,

- Incorporation of more mission loads with accompanying energy storage,

- Consideration of alternative disruption distributions in which the disruption may be more likely to affect centralized energy storage modules,

- Study of the impact of energy storage decisions on maneuvering and available propulsion power,

- Investigation of the feasibility of transitioning this approach,

- Assessment of effect of use of reduced-order models [4] on results,

- Investigation of fault management strategies in MVDC systems in terms of mission performance and volume, and

- Study of power management strategies for systems with significant energy storage capability.

References

[1] J. Borraccini, "Machinery system alternatives based on mission load elasticity."

[2] J. S. Chalfant and C. Chryssostomidis, "Analysis of various all-electric-ship electrical distribution system topologies," in *2011 IEEE Electric Ship Technologies Symp.*, Alexandria, VA, pp. 72–77.

[3] J. S. Chalfant, C. Chryssostomidis, and M. G. Angle, "Study of parallel ac and dc electrical distribution in the all-electric ship," in *Proc. Grand Challenges Modeling Simulation*, Ottawa, Canada, pp. 319–326, 2010.

[4] A. M. Cramer, H. Chen, and E. L. Zivi, "Shipboard electrical system modeling for early-stage design space exploration," in *IEEE Electric Ship Technologies Symp., 2013*, Arlington, VA, pp. 128–134.

[5] J. W. Kolar, U. Drofenik, J. Biela, M. L. Heldwein, H. Ertl, T. Friedli, and S. D. Round, "PWM converter power density barriers," in *Power Conversion Conf. – Nagoya, 2007*, Japan, pp. 9–29.

[6] A. M. Cramer, S. D. Sudhoff, and E. L. Zivi, "Performance metrics for electric warship integrated engineering plant battle damage response," *IEEE Trans. Aerosp. Electron. Syst.*, vol. 47, no. 1, pp. 634–646, Jan. 2011.

[7] A. M. Cramer, S. D. Sudhoff, and E. L. Zivi, "Metric optimization-based design of systems subject to hostile disruptions," *IEEE Trans. Syst., Man, Cybern. A, Syst., Humans*, vol. 41, no. 5, pp. 989–1000, Sep. 2011.

Appendix 3

A. M. Cramer, F. Pan, H. Chen, and E. L. Zivi, "Modeling and simulation for early-stage quantitative assessment of medium-voltage dc power system protection schemes," in *Electric Machines Technology Symp. 2014*, Philadelphia, PA, 28-29 May, 2014.

Modeling and Simulation for Early-Stage Quantitative Assessment of Medium-Voltage DC Power System Protection Schemes

Aaron M. Cramer, Fei Pan, Hanling Chen
Department of Electrical and Computer Engineering
University of Kentucky
Lexington, KY, USA
Email: aaron.cramer@uky.edu, fei.pan@uky.edu, hanling.chen@uky.edu

Edwin L. Zivi
Weapons and Systems Engineering Department
United States Naval Academy
Annapolis, MD, USA
Email: zivi@usna.edu

Abstract—Short-circuit protection is one of the greatest risks associated with a transition towards medium-voltage dc (MVDC) shipboard power systems. While ac circuit breakers and associated protection schemes are well-understood, there are remaining technical challenges associated with the protection of MVDC systems. Technologies such as dc circuit breakers and fault current limiters are not as mature as their ac counterparts. Herein, a method for extending a successful early-stage modeling approach in order to assess alternative MVDC protection schemes quantitatively is described. This method will generalize the existing approach to consider the effect of the behavior of breakers and sectionalizers on the ability of the power system to provide power through both accidental faults and those resulting from damage. This entails modifications to the bus model to account for nonideal sectionalizing behavior and modifications to the generator model to address temporary generator bus faults. This approach is demonstrated using a notional power system model.

I. INTRODUCTION

The power system of an electric warship can be viewed as a service provider that is responsible for providing electric power to the mission loads that it serves [1]–[3]. Thus, it has been established that the dynamic assessment of the power system should be performed with respect to its ability to deliver this power across the variety of scenarios in which it must operate [2], [4]. A variety of time-domain performance metrics have been discussed for evaluating the performance of the power system [2], [4]. As the system must perform well under a broad range of scenarios, many simulations are necessary in order to assess the system's performance over these scenarios. This motivates the development of modeling and simulation techniques that minimize the computational burden of these simulations. It has been found that the electrical dynamics of the system have relatively little influence on the performance of the system as long as the system has been well designed (e.g., stable) [4]–[7]. Therefore, the computational burden of the simulations can be reduced by neglecting the electrical dynamics of the system [4], [5], [8]. Linear programming approaches have previously been proposed and successfully demonstrated in [5], [8]. In these approaches, the mechanical dynamics associated with prime movers and energy storage

dynamics are retained, but the electrical power flow is modeled statically.

The ability to perform such studies early in the design process is very useful for identifying technical risks. It is widely understood that short-circuit protection is one of the greatest risks associated with a transition towards medium-voltage dc (MVDC) shipboard power systems [9], [10]. While ac circuit breakers and associated protection schemes are based on mature technology, there are remaining technical challenges associated with the protection of MVDC systems. The ability to use previously successful early-stage modeling techniques to investigate these issues is clearly advantageous.

Neglect of electrical dynamics has proven very useful for early-stage design space exploration [4]–[6], [8]. However, these approaches are motivated by the modeling of permanent faults; they have significant shortcomings when modeling temporary faults and nonideal protection system behavior. Herein, these shortcomings are addressed by modifying the network and generator representations used in the linear programming approach. The remainder of this paper is organized as follows. In Section II, the required modeling modifications are presented. Then, the notional MVDC system used to demonstrate the method is described in Section III. The proposed method is demonstrated in Section IV and conclusions and directions for future research are presented in Section V.

II. MODELING

Linear-programming approaches to modeling the electric power system neglect the electrical dynamics of the system and approximate the behavior of the system using a linear program that must be solved at each time step. The structure of the linear program is as follows:

$$\max_{\mathbf{x}} \quad \mathbf{c}^{\mathrm{T}}\mathbf{x}$$
$$\text{subject to} \quad \mathbf{A}\mathbf{x} \le \mathbf{b}$$
$$\mathbf{A}_{eq}\mathbf{x} = \mathbf{b}_{eq}$$
$$\mathbf{x} \le 0.$$

In this linear program, the elements of the vector $\mathbf{x}$ represent the decision variables that describe the power flows within the system. The matrices $\mathbf{A}$ and $\mathbf{A}_{eq}$ and the vectors $\mathbf{b}$ and $\mathbf{b}_{eq}$ describe the network relationships and constraints. The vector $\mathbf{c}$ describes the weight of different power flows in order to approximate optimal power allocation. Full details of the structure of the linear program can be found in [8].

In order for the model presented in [5], [8] to be used to study the effects of faults and the behavior of circuit protection devices, the model must be modified. In particular, in [5], [8] ideal sectionalizing behavior is assumed for line and bus faults. This leads to highly idealized predictions of the response of the system to such faults. Another area in which the model must be modified is to account for the behavior of generators during temporary faulted conditions. In [5], [8], a temporary fault leads to the generator becoming permanently unavailable. These models were intended to study permanent faults and they also assumed ideal sectionalizing behavior, so this limitation was not unreasonable. However, in order to faults and system protection, these limitations must be alleviated. This requires modifications to the electrical network model and to the generator model as described below.

A. Bus, Interconnect, and Line

Each bus in the system can be faulted due to damage (as described previously in [8]) or due to an accidental fault. While faults due to damage are considered permanent (on the time scale of interest), accidental faults may be temporary or permanent. In particular, the internal fault status is described by

$$f_{internal} = h + f_{imposed}$$

where h is the hit status of the bus (e.g., calculated by [11]) and $f_{imposed}$ is the imposed fault status of the bus, used to simulate an accidental fault of the bus, and $+$ is the logical or operator.

An interconnect represents a point at which two buses (a "from" bus and a "to" bus) may be disconnected. The switch status s of the interconnect is used to describe whether a fault on one of the buses causes the other bus to be faulted. In [8], the sectionalizing behavior of interconnects was assumed to be ideal. In other words, if a fault occurred on one bus, the other bus was instantly disconnected and unaffected by the fault. Herein, the interconnect is assumed to open if one of the buses has an internal fault, but this occurs after a clearing time Δt_{clear}.

A line represents the connection between a component and a bus. Each line can be faulted due to damage or due to an accidental fault. Similarly to the internal fault status of the bus, the internal fault status of a line is described by

$$f_{internal} = h + f_{imposed}$$

where h is the hit status of the line and $f_{imposed}$ is the imposed fault status of the line. Each line is assumed to have a switch that is capable of isolating the line from the bus in the case that the line is faulted. The switch status s of the

line indicates whether a fault on the line causes the bus to be faulted. Some buses are isolated from line faults through the use of components such as auctioneering diodes. Faults on such lines will not propagate to adjacent buses. These lines are labeled unidirectional, and they always have a false switch status. This does not indicate that the lines do not transmit power; rather, they do not propagate faults. For other lines, the switch is assumed to open if the line has an internal fault, but this occurs after some clearing time Δt_{clear}.

With the internal fault status of buses and lines and the switch status of interconnects and lines defined, it is possible to formulate the fault status of each bus and line. In particular, if a bus or line has an internal fault, then it is faulted:

$$f_{internal} \rightarrow f$$

where f is the fault status of the component. If a line is faulted and its switch is closed, the bus is faulted:

$$f_{line} \cdot s_{line} \rightarrow f_{bus}$$

where $\cdot$ is the logical and operator. If an interconnect is closed and either bus is faulted, the other bus is faulted:

$$s_{interconnect} \cdot f_{from\ bus} \rightarrow f_{to\ bus}$$
$$s_{interconnect} \cdot f_{to\ bus} \rightarrow f_{from\ bus}$$

Finally, if a bus is faulted, the line is faulted:

$$f_{bus} \rightarrow f_{line}.$$

Having calculated the bus status of each bus and line, it is possible to adjust the system linear program to account for the faults. In particular, power cannot flow to or from a faulted bus.

B. Generator

Gensets have limited slew rates that are generally related to prime mover dynamics. This was represented in [5], [8] by constructing a set of differential equations describing the minimum and maximum generator output power at each moment in time. If the state of the electrical distribution system and loads was such that the generator could not deliver the minimum power (e.g., due to fault or sudden load shed), the generator was considered to go off line due to an overspeed condition. This representation is not well suited to systems in which generator buses may experience temporary faults. In such cases, any main bus fault would cause all of the generators to go off line. Furthermore, no provision existed for the generators to return to service following such faults.

Herein, an alternative generator model is proposed. In this generator model, the prime mover dynamics are represented using a simple model. In particular, if ϵ represents the normalized speed error of the generator, then its dynamics can be represented by

$$2H\frac{d\epsilon}{dt} = \frac{P_m - P}{P_{rating}}$$

where P is the output power of the generator, P_m is the mechanical power being applied by the prime mover, P_{rating}

is the rated output power of the generator, and H is the inertia constant of the generator. Furthermore, the dynamics of the prime mover can be expressed as

$$\frac{dP_m}{dt} = \text{bound}\left(\frac{P - P_m}{\tau} - \beta\epsilon, -pP_{slew}, pP_{slew}\right)$$

where pP_{slew} is the maximum slew rate of the prime mover's mechanical power, τ is a time constant, β is a control gain, and

$$\text{bound}(x, a, b) = \begin{cases} a & x < a \\ x & a \leq x \leq b \\ b & x > b. \end{cases}$$

Therefore, at each point in time, the minimum and maximum allowable generator power can be formulated as

$$P_{min} = P_m - \sqrt{4HpP_{slew}(\epsilon_{max} - \epsilon)} \qquad (1)$$

$$P_{max} = P_m + \sqrt{4HpP_{slew}(\epsilon_{max} + \epsilon)} \qquad (2)$$

where ϵ_{max} is the maximum allowable normalized speed error. It can be shown that if the generator's output power remains within these two limits, the absolute normalized speed error will remain in the allowable range. The square roots in (1) and (2) should be continuously extended in the case that their arguments are negative. In particular, a signed square root is appropriate:

$$\begin{cases} \sqrt{x} & x \geq 0 \\ -\sqrt{-x} & x < 0. \end{cases}$$

While the generator is operational, its output power should be limited such that

$$\max\{P_{min}, 0\} \leq P \leq \min\{P_{max}, P_{rating}\}.$$

It has been shown in [8] that the linear programming approach can enforce the upper limit on the output power. However, there are cases in which the lower limit cannot be enforced due to faults or sudden load sheds. To handle this case, a heavily penalized variable is used to allow the output power to fall below the minimum level. When this happens, the generator speed will increase. When $\epsilon > \epsilon_{max}$, the generator becomes inoperable due to overspeed status. While off line, the generator's output power is zero. The generator resumes operation when $P_{min} \leq 0$ and $P_{max} \geq 0$ or when $P_{min}P_{max} < 0$. This model allows the generator to experience temporary bus faults without tripping and to resume operation when the generator speed recovers.

III. NOTIONAL SYSTEM MODEL

The proposed modeling approach is demonstrated using a notional system based on the Electric Ship Research and Development Consortium notional MVDC system as described in [7], [12]. A simplified representation of the system is shown in Fig. 1. In this system, two types of generators exist: main generators (MTGs) and auxiliary generators (ATGs). The parameters of these generators are given in Table I. The propulsion drives (PMD) have a power rating of 29.4 MW and an efficiency of 98%. The maximum total propulsion load is
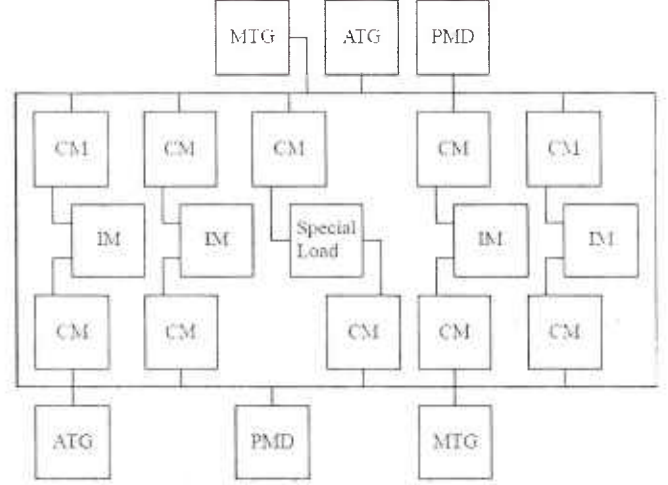

Fig. 1. Notional MVDC system. MTG signifies main generator, ATG signifies auxiliary generator, PMD signifies propulsion drive, CM signifies a dc-dc converter, IM signifies a converter to end-use form

TABLE I
GENERATOR PARAMETERS

Parameter	MTG	ATG
P_{rating} (MW)	36	5
pP_{slew} (MW/s)	0.8	0.8
H (s)	6	6
ϵ_{max}	0.01	0.01
τ (s)	0.5	0.5
β (MW/s)	288	40

58.9 MW. The dc-dc converters (CMs) each have an efficiency of 99%. The CMs serving the special load have a power rating of 3.75 MW, the maximum special load. The CMs serving the zonal loads have a power rating of 1.26 MW. The end-use converters (IMs) have an efficiency of 99% and a power rating of 2.08 MW. Each zone contains energy storage modules with a capacity of 242 MW, a power capability of 2.02 MW, and a charging/discharging efficiency of 99%. Each zone contains an aggregate vital load of 930 kW and an aggregate nonvital load of 840 kW.

In order to formulate the linear program, weights are necessary for the various power flows. In particular, the generator output power is weighted at 0.5. The propulsion power is divided into several ranges with different weights as shown in Table II. The special load has a weight of 15. The energy storage modules have a charging weight of 2 and a discharging weight of 10. The vital loads have a weight of 25, and the nonvital loads have a weight of 3.

IV. SIMULATION RESULTS

The system is simulated from zero initial conditions for 15 minutes. This simulation requires 3.09 s of run time on a 2.79 GHz Intel Core i7 processor with 4 GB of RAM using MATLAB's ode23tb solver, so the modeling approach retains the computational efficiency associated with neglecting the

Power (MW)	Weight
0.198	26
1.18	18
3.20	16
6.14	14
12.8	6
35.4	1

Fig. 2. Simulation of startup transient.

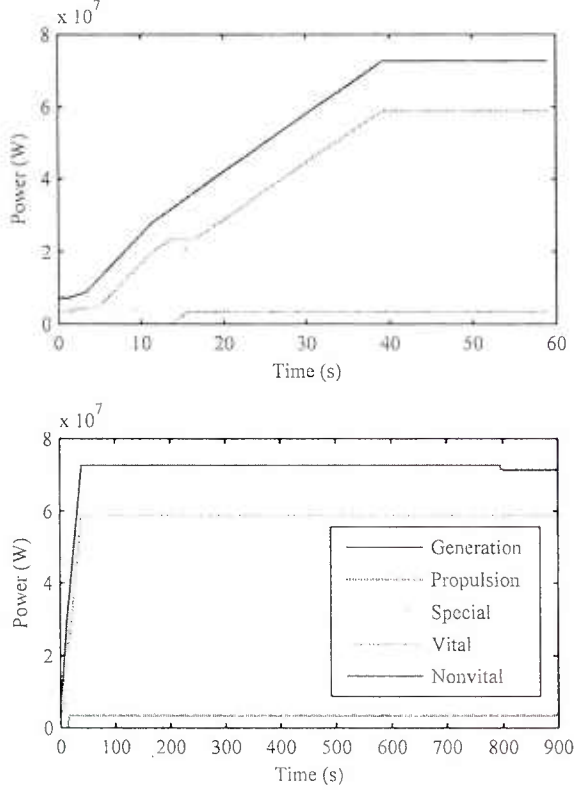Fig. 3. Simulation of bus fault cleared in 0.2 s.

Fig. 4. Simulation of bus fault cleared in 0.05 s.

electrical dynamics. The generated power as well as the power consumed by the various types of load are shown in Fig. 2. It can be seen that as the generator prime movers ramp up, power is initially allocated to propulsion and the vital loads. At about 3 s, the special load begins to be served. Once the special load is satisfied, more power is allocated to propulsion starting at 4.8 s. At 13.5 s, the nonvital loads begin to be served. The load allocated to propulsion continues to increase until it reaches its maximum at 39 s. Finally, at 796 s, the generated power decreases as the energy storage modules are completely filled. This simulation shows the startup transient and establishes the steady-state condition of the system.

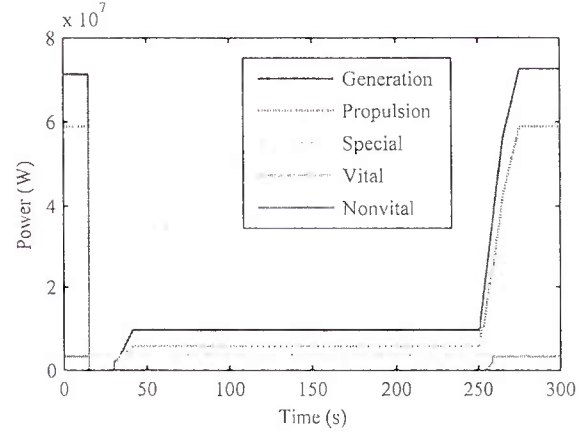Starting from the steady-state condition reached at the end of 15 minutes, two fault cases are considered. In the first, a temporary bus fault (lasting 5 s) on one of the b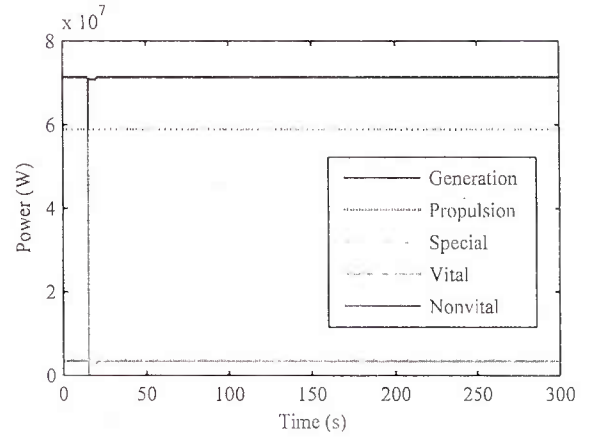uses occurs and is cleared in 0.2 s. The results are shown in Fig. 3. It can be seen that the all of the generators trip. The vital load in each zone is satisfied with energy storage. About 15 s after the fault, the ATGs recover and begin to serve the most important loads. At about 236 s after the fault, the MTGs recover and the system begins to return to its original operating condition. This study takes 3.75 s of runtime. In the second case, a the same bus fault occurs, but the clearing time is reduced to 0.05 s (3 60-Hz cycles). The results of this case are shown in Fig. 4. It can be seen that the fault causes a momentary outage of some loads and that the system quickly resumes operation after the temporary fault is cleared. This study requires 0.43 s of runtime, illustrating that the runtime in such cases is more a function of the complexity of the event than the duration of time being simulated.

V. CONCLUSIONS AND FUTURE RESEARCH

The proposed modifications to the linear programming approach to modeling shipboard power systems allow it to be used to study both permanent and temporary faults. This facilitates the investigation of circuit protection design questions

using the early-stage modeling approach. There are remaining issues associated with the representation of the power control system. The weights that are used in the linear programming method are based on mission prioritization, and the use of such weights is appropriate when considering faults due to hostile disruption. However, following temporary nuisance faults, quality-of-service requirements must be considered [13], [14]. This can be handled by using time-varying load weights. Specifically, each load may have a quality-of-service weight and a mission weight. By varying between these weights, it is possible to represent the behavior of a power controller balancing quality-of-service and mission requirements, and this is a direction of future work.

REFERENCES

[1] J. P. Walks and J. F. Mearman, "Integrated engineering plant," presented at the Amer. Soc. Naval Engineers Reconfiguration Survivability Symp. 2005, Atlantic Beach, FL.

[2] A. M. Cramer, S. D. Sudhoff, and E. L. Zivi, "Performance metrics for electric warship integrated engineering plant battle damage response," *IEEE Trans. Aerosp. Electron. Syst.*, vol. 47, no. 1, pp. 634–646, 2011.

[3] M. G. Richards, D. E. Hastings, D. H. Rhodes, and A. L. Weigel, "Defining survivability for engineering systems," in *Proc. 5th Annu. Conf. Syst. Eng. Res.*, 2007.

[4] A. M. Cramer, S. D. Sudhoff, and E. L. Zivi, "Metric optimization-based design of systems subject to hostile disruptions," *IEEE Trans. Syst., Man, Cybern. A, Syst., Humans*, vol. 41, no. 5, pp. 989–1000, 2011.

[5] R. R. Chan, S. D. Sudhoff, Y. Lee, and E. L. Zivi, "A linear programming approach to shipboard electrical system modeling," in *IEEE Electric Ship Technologies Symp., 2009*, Baltimore, MD, pp. 261–269.

[6] R. R. Chan, S. D. Sudhoff, and E. L. Zivi, "An approach to optimally allocate energy storage in naval electric ships," in *2011 IEEE Electric Ship Technologies Symp.*, Alexandria, VA, pp. 402–405.

[7] J. S. Chalfant and C. Chryssostomidis, "Analysis of various all-electric-ship electrical distribution system topologies," in *2011 IEEE Electric Ship Technologies Symp.*, Alexandria, VA, pp. 72–77.

[8] A. M. Cramer, H. Chen, and E. L. Zivi, "Shipboard electrical system modeling for early-stage design space exploration," in *IEEE Electric Ship Technologies Symp., 2013*, Arlington, VA.

[9] N. Doerry, "Next generation integrated power system: NGIPS technology development roadmap," Naval Sea Systems Command, Washington, DC, Tech. Rep., Nov. 2007.

[10] J. Kuseian, "Naval power systems technology development roadmap," Naval Sea Systems Command, Washington, DC, Tech. Rep., May 2013.

[11] A. M. Cramer, R. R. Chan, S. D. Sudhoff, Y. Lee, M. R. Surprenant, N. S. Tyler, E. L. Zivi, and R. A. Youngs, "Modeling and simulation of an electric warship integrated engineering plant," in *SAE Power Systems Conf.*, New Orleans, LA, Nov. 2006.

[12] J. S. Chalfant, C. Chryssostomidis, and M. G. Angle, "Study of parallel ac and dc electrical distribution in the all-electric ship," in *Proc. Grand Challenges Modeling Simulation*, Ottawa, Canada, 2010.

[13] N. Doerry and D. Clayton, "Shipboard electrical power quality of service," in *IEEE Electric Ship Technologies Symposium*, Jul. 2005, pp. 274–279.

[14] N. Doerry, "Designing electrical power systems for survivability and quality of service," *Nav. Eng. J.*, vol. 119, no. 2, pp. 25–34, 2007.